



DISSERTATION APPROVAL SHEET

Title of Dissertation: A Generalized Model of Flocking with Steering

Name of Candidate: Guy Djokam

Doctor of Philosophy, 2021

Graduate Program: Applied Mathematics

Dissertation and Abstract Approved:

Muruhan Rathinam

Muruhan Rathinam

Professor

Mathematics and Statistics

11/25/2021 | 2:48:35 PM EST

NOTE: *The Approval Sheet with the original signature must accompany the thesis or dissertation. No terminal punctuation is to be used.

ABSTRACT

Title of dissertation: A Generalized Model of Flocking with Steering

Guy Aime Djokam, Doctor of Philosophy, 2021

Dissertation directed by: Professor Muruhan Rathinam
Department of Mathematics and Statistics

Flocking is a phenomenon in which self-propelled agents use only simple rules based on information about the locations and velocities of other agents to move from an unordered motion to an ordered motion in the long run. In the literature, many authors have extensively studied this phenomenon.

In this dissertation, we introduce a model for the dynamics of flocking with steering of a finite number of agents. In this model, each agent's acceleration consists of flocking and steering terms. The flocking term is a generalization of many of the existing models and allows for the incorporation of real-world features such as acceleration bounds, partial masking effects, and orientation bias. The steering term models the individualistic behavior of agents and allows them to compensate for other external forces such as friction and gravity. The analysis of the obtained model provides sufficient conditions under which agents flock and steer together. Our analysis shows that the asymptotic velocity need not be a constant vector. It is rather a function of time determined by the steering terms.

Motivated by the idea that staying together as a flock is more important than pursuing the individual whims of agents, we use singular perturbation theory to study our model when the flocking accelerations are much faster than the steering accelerations. Our analysis shows that the leading order behavior is one where the agents have a common flocking velocity which evolves according to a differential equation. We also provide a limited but rigorous analysis over a finite time horizon and study the limiting behavior as a critical parameter ϵ approaches zero. Here, ϵ is the time scale separation between the fast flocking and the slow steering.

Additionally, we numerically explore the inclusion of repulsive forces into our model in order to avoid collisions. Our simulations suggest that with an appropriate choice of parameters, collisions may be prevented while retaining the flocking behavior.

A Generalized Model of Flocking with Steering

by

Guy Aime Djokam

Dissertation submitted to the Faculty of the Graduate School of the
University of Maryland, Baltimore County in partial fulfillment
of the requirements for the degree of
Doctor of Philosophy
2021

Advisory Committee:

Dr. Muruhan Rathinam, Chair/Advisor

Dr. Hye Won Kang

Dr. Evelyn Sander

Dr. Jinglai Shen

Dr. Justin Webster

© Copyright by
Guy Aime Djokam
2021

Dedication

To my mother Regine Ngako epse Hadjeu, my late father Michel Hadjeu, my daughters Tcheupi Djokam and Hadjeu Djokam, and to my siblings.

Acknowledgments

I owe my gratitude to all the people who have made this dissertation possible and because of whom my graduate experience has been one that I will cherish forever.

First and foremost I would like to thank my advisor, Professor Rathinam for giving me an invaluable opportunity to work on challenging and interesting topic over the past four years. He has always made himself available for help and advice and there has never been an occasion when I've solicited his help and he hasn't given me time. Even with this pandemic that has changed our lifestyle, he has always found a way to help. His guidance helped me all the time of my research and writing of this dissertation. It has been a pleasure to work with and learn from such an extraordinary individual. I would like to thank Dr. Jinglai Shen and Dr. Justin Webster, Dr. Hye Won Kang, and Dr. Evelyn Sander for serving as advisory committee. I would like to thank Professor Animikh Biswas to facilitate my admission to the graduate program at UMBC. I then extend my gratitude to all professors at the graduate level in mathematics at UMBC.

My sincere gratitude also goes to Dr. Roman Sznajder and Dr. Mehran Mahdavi at Bowie State University for their teaching and motivation to pursue a Ph.D. program in Mathematics. After being out of school for a long time I am so grateful for the knowledge I received in Real Analysis, Numerical Analysis, Differential Equations, and Complex Analysis at Bowie State University. Lastly, I

would like to thank my daughters Tcheupi Djokam and Hadjeu Djokam who always inspire me, and most of the time, they will go to bed very late because they are waiting for Daddy.

It is impossible to remember all, and I apologize to those I've inadvertently left out. Lastly, thank you all, and thank God!

Contents

List of Figures	vii
List of Abbreviations	ix
1 Introduction	1
1.1 Literature Review	1
1.2 Our Contribution	7
2 Generalization of the Model	10
2.1 Apriori Acceleration Bounds	11
2.2 Masking Effect and Orientation Bias	12
2.3 The Open Loop and Closed Loop Models	19
2.4 Inclusion of Friction	20
2.5 Ring Mill Phenomena	21
2.6 Steering	24
2.7 Existence and Uniqueness	25
3 Analysis of the Model	27
3.1 Preliminaries	27
3.2 Analysis of the Open Loop	29
3.3 Analysis of the Closed Loop	33
4 Fast Flocking with Slow Steering	38
4.1 Leading Order Behavior	39
4.2 Initial Transient Layer	45
4.3 Numerical examples	48
4.3.1 Choice of the Parameters γ_1 and γ_2	49
4.3.2 Simulations	54
4.4 Analysis of the Singularly Perturbed Model	64
5 A Generalized Model With Steering and Collision Avoidance Terms	68
5.1 Simulations of the Model with Extra Force Derived from Morse Potential	69

5.2	Simulation of the Model with Inter-particle Bonding Forces	74
6	Conclusion	79
A	Useful Lemmas	82

List of Figures

2.1	<i>Masking effect and orientation bias. The agents j and k are equidistant from agent i. Nevertheless, agent l contributes to the masking effect which diminishes agent j's influence on agent i. On the other hand, agent i is moving to the right and in agent, i's field of view agent j is in a more prominent position than agent k, which diminishes agent k's influence on agent i.</i>	14
2.2	<i>θ is the angle at i and ψ is the angle at j. This graph explains the construction of w_{ijl}.</i>	15
2.3	Effect of factor $\exp\{-h(w_{123} + w_{213})\}$ for two points $x_1 = (1, 0)^t$ and $x_2 = (2, 0)^t$ and the third element is in the domain $[0.8, 2.2] \times [-0.5, 0.5]$	17
2.4	Effect of factor $\exp\{-h(w_{123} + w_{213})\}$ for two points $x_1 = (1, 0)^t$ and $x_2 = (2, 0)^t$ and the third element is in the domain $[0.8, 2.2] \times [-0.5, 0.5]$ see from above	18
3.1	<i>Illustration of the lemma</i>	30
4.1	y_1 in red, y_2 in green and y_3 in blue	53
4.2	Trajectories in position and velocity spaces. Cyan circles represent initial values and red stars the final values. Case $\epsilon = 0.1$.	55
4.3	Positions against time. Case $\epsilon = 0.1$. Target trajectory in dash black.	56
4.4	Velocities against time. Case $\epsilon = 0.1$. Target velocity in dash black	56
4.5	Velocities against time for t close to zero. Case $\epsilon = 0.1$ short representation. Target velocity in dash black	57
4.6	Trajectories in position and velocity spaces. Cyan circles represent initial values and red stars the final values.. Case $\epsilon = 0.01$.	57
4.7	Trajectories against time. Case $\epsilon = 0.01$. Target trajectory in dash black	58
4.8	Velocities against time. Case $\epsilon = 0.01$. Target velocity in dash black	58
4.9	Velocities against time for t close to zero. Case $\epsilon = 0.01$. Target velocity in dash black	59
4.10	Trajectories in position and velocity spaces. Cyan circles represent initial values and red stars the final values.. Case $\epsilon = 0.001$.	60
4.11	Positions against time. Case $\epsilon = 0.001$. Target trajectory in dash black	60

4.12	Velocities against time. Case $\epsilon = 0.001$. Target velocity in dash black	61
4.13	Velocities against time for t close to zero. Case $\epsilon = 0.001$. Target velocity in dash black	61
4.14	Comparison between the reduced model (in green) and exact solution (in blue) for $\epsilon = 0.1$	62
4.15	Comparison between the reduced model (green) and exact solution (in blue) for $\epsilon = 0.01$	63
4.16	Comparison between the reduced model (in green) and exact solution (in blue) for $\epsilon = 0.001$	63
5.1	Morse potential graph	70
5.2	Comparison of solutions $x_i(t)$ and $v_i(t)$: Case of Morse potential . . .	72
5.3	Comparison minimum distance between agents: case of Morse potential(green), case without repulsion (blue)	73
5.4	Comparison of solution x_i and v_i : Case of inter-particle bonding forces	75
5.5	Comparison of minimum distance when the inter-particle bonding force is added.	75
5.6	Comparison of the configuration diameters of the model: Diameter without a repulsive force (blue). Diameter with Morse Potential(red). Diameter with inter-particle bonding forces(orange)	78
5.7	Comparison of diameters velocity of the model: Diameter without a repulsive force (blue). Diameter with Morse Potential(red). Diameter with inter-particle bonding forces(orange)	78

List of Abbreviations and Symbols

CS	Cucker and Smale
MT	Motsch and Tadmor
NASA	National Aeronautics and Space Administration
γ, Γ	gamma
λ, Λ	lambda
α	alpha
β	beta
θ	theta
MP	Morse Potential
ξ	xi
ϕ	phi
ψ	psi
σ	sigma
\sum	sum
C^1	continuously differentiable function

Chapter 1: Introduction

1.1 Literature Review

Self-organized motion such as flocking of birds is a phenomenon in which self-propelled agents use only simple rules based on information about the locations and velocities of other agents to move from an unordered motion to an ordered motion in the long run. This phenomenon can be observed in many domains. Natural occurrences include the flocking of birds, the schooling of fish, the herding of sheep, and the swarming of bacteria. Due to its applications in many engineering areas, such as mobile sensor networks and cooperative robots, several investigations have examined this process across various disciplines such as control theory, physics, and applied mathematics. For instance, see [2], [3], [9], [14], [18], [21], [25], [29], [32].

In the scientific community, many models have been created to interpret, understand or influence self-organized phenomena. In 1987 (see [29]), based on his observation of how birds flock, Reynolds created a computer program of flocking phenomena. His algorithm was based on three simple rules: cohesion, collision avoidance, and alignment. Cohesion means that a bird will regard the position of

the nearby birds and try to stay close to their average position. Collision avoidance means that a bird will regard the distance to nearby birds and that if they are too close, a bird will steer away to avoid collision. Alignment means that a bird will match its velocity to the nearby bird. In short, each bird adjusts its behavior based on its neighbor's behavior. The computer program was later adopted by NASA researchers (Dryden Flight Research Center) to demonstrate the coordination of two unmanned aircraft in 2005 [10].

Vicsek and colleagues proposed [32] a simple model that investigates the emergence of self-ordered motion in systems of particles with biologically motivated interactions. The model consisted of N particles moving with the same speed but in different headings. The Vicsek model is discrete in time and at each step, the velocity and the position of particle i is simultaneously determined by the formula

$$x_i(t + \delta t) = x_i(t) + v_i(t)\delta t$$

in which the velocity of particle i at time $(t + \delta t)$ is constructed to have the same magnitude of the velocity v at time t and the heading is given by

$$\theta(t + \delta t) = \langle \theta(t) \rangle_r + \delta\theta.$$

Herein, $\delta\theta$ is a random number chosen with uniform probability from the interval $[-\eta/2, \eta/2]$ where $0 < \eta \ll 1$. And $\langle \theta(t) \rangle_r$ is the average heading of particles in the neighborhood of particle i . The authors show via simulation that all particles will move in the same direction when the density $\rho = \frac{N}{L^2}$ is high and the noise is small (L

is the size of the square that contains the N agents). Using the graph representation of the Vicsek model and graph properties, the authors in [22] proved that the model converges asymptotically to a fixed configuration. This model presents some limitations, most notably that the magnitudes of velocities of agents is assumed constant in time.

Inspired by the Vicsek model, Cucker and Smale (CS) (see [12]) proposed a continuous model in which the magnitude of the velocity is not constant. The dynamical equation of the CS model is given by

$$\begin{aligned}\dot{x}_i &= v_i \\ \dot{v}_i &= \frac{1}{N} \sum_{j=1}^N \phi(\|x_i - x_j\|)(v_j - v_i).\end{aligned}\tag{1.1.1}$$

Here, x_i and v_i are functions of time. They denoted the position and velocity of agent i . N is the number of agents, $a_{ij} = \phi(\|x_i - x_j\|)$ is the influence of agent j on agent i . The influence function ϕ is positive and non-increasing. This model was very successful as many authors contributed to its analysis [1], [5], [11]–[13], [16], [18], [23], [24], [27], [30]. The general form of the influence function in the Cucker Smale type model is:

$$\phi(r) = \frac{K}{(a^2 + r^2)^\beta}, \text{ where } K > 0 \text{ and } a > 0.$$

It was shown that there is unconditional flocking if $\beta < 1/2$. When $\beta \geq 1/2$ the flocking state depends on some conditions on initial data. The critical case $\beta = 1/2$ was proven to be unconditional in [18] in which the authors construct some explicit

Lyapunov functional. Moreover, the authors give an elegant proof of convergence of the Cucker Smale model. In the Cucker Smale model, the influence function is symmetric which led to the result that the asymptotic velocity $v^f = \frac{1}{N} \sum_{i=1}^N v_i(0)$. Many models were derived from the CS model. For instance, in [16] the authors proposed a model in which the linear factor $v_j - v_i$ is replaced by a non linear factor $\Gamma(v_j - v_i)$ in the acceleration term. That is,

$$\begin{aligned}\dot{x}_i &= v_i \\ \dot{v}_i &= \frac{1}{N} \sum_{j=1}^N \phi(\|x_i - x_j\|) \Gamma(v_j - v_i).\end{aligned}\tag{1.1.2}$$

Here, $\Gamma : \mathbb{R}^d \rightarrow \mathbb{R}^d$ is continuous and satisfies the following assumptions.

- Skew symmetric $\Gamma(v) = -\Gamma(-v) \forall v \in \mathbb{R}^d$.
- (Coercivity) There exists some constant $c_1 > 0$ and $\gamma \in (1/2, 3/2)$ such that,

$$\langle \Gamma(v), v \rangle \geq c_1 \|v\|^{2\gamma}.$$

Note that the CS model does not guarantee cohesion nor does it prevent a collision.

Some researchers attempted to resolve these issues. For instance, the authors in [27]

via heuristic argument proposed the following model:

$$\begin{aligned}\dot{x}_i &= v_i \\ \dot{v}_i &= \frac{1}{N} \sum_{j=1}^N \phi(\|x_i - x_j\|) (v_j - v_i) \\ &\quad + \frac{\sigma}{N} \sum_{j=1}^N \frac{K_1}{2r_{ij}^2} \langle v_i - v_j, x_i - x_j \rangle (x_j - x_i) + \frac{\sigma}{N} \sum_{j=1}^N \frac{K_2}{2r_{ij}} (r_{ij} - 2R) (x_j - x_i).\end{aligned}\tag{1.1.3}$$

Where, σ , K_1 , R and K_2 are constant parameters and $r_{ij} = \|x_i - x_j\|$. For this model, the authors show that flocking occurs under some conditions involving initial data and the influence function ϕ . Another idea to avoid a collision was proposed in [11]. Here the acceleration is augmented by the term $\frac{1}{N} \sum_{j=1}^N f(\|x_i - x_j\|^2)(x_i - x_j)$. The function f is a positive measurable function such that there exist $d_0 > 0$ satisfying,

$$\int_{d_0}^{d_0+1} f(r)dr = \infty \quad \text{and} \quad \int_{d_0}^{\infty} f(r)dr < \infty.$$

Even though the result of the analysis of the CS model is theoretical, the result was applied in spacecraft flight control in the context of the European Space agency DARWIN mission [28].

In [25], the authors presented some drawbacks of the CS model. For instance, the CS model flocks to the average velocity of the initial velocity of all agents. The influence function is symmetric which is not realistic. To solve these issues, Motsch and Tadmor proposed the following model

$$\begin{aligned} \dot{x}_i &= v_i \\ \dot{v}_i &= \alpha(\bar{v}_i - v_i). \end{aligned} \tag{1.1.4}$$

Where $\bar{v}_i = \sum_{j=1} a_{ij} v_j$ and $a_{ij} = \frac{\phi(\|x_i - x_j\|)}{\sum_k \phi(\|x_i - x_k\|)}$ is the influence of agent j on agent i . This new form of influence function is not symmetric which is a key point of the analysis of the CS model. To analyze this new model, the authors developed new tools such as the notion of active sets, and the maximal action of an anti-symmetric matrix. Combining these ideas with the technique developed in [18], the authors

show that the new model flocks under certain conditions depending on the initial data. Moreover, they prove that the flocking velocity is in the convex hull defined by the initial velocities.

In the literature [6], [8], [14], [28], we have another type of flocking model given by

$$\begin{aligned}\dot{x}_i &= v_i \\ \dot{v}_i &= (\alpha - \beta \|v_i\|^2)v_i - \nabla(W_i(x)).\end{aligned}\tag{1.1.5}$$

Here $x_i, v_i \in \mathbb{R}^d$ are position and velocity vector of agent i . α and β are strict positive parameters that define self propulsion and friction coefficients. The function

$$W_i(x) = \sum_{j \neq i} U(\|x_i - x_j\|),$$

is the attraction-repulsion potential that are acting on agent i . In [14] the authors D'Orsogna et al use the Morse potential for U . There exist solutions where $v_i(t) = v^\infty$ a constant for all i and for all t in which $\|v^\infty\| = \sqrt{\frac{\alpha}{\beta}}$. Many authors have analyzed this type of model from different perspectives see [3], [9], [14], [15]. In [14], authors have studied pattern formation. They have also studied the stability of flock, and ring mills. Flock mill is when all agents are regularly positioned on a circle of fixed radius and move in a translational motion with same velocity v^∞ . Ring mill is when agents have circular motion on circle of radius R with constant angular velocity. In [9], these equations are extended by including an additional force, called the roosting force, describing an attraction to a roosting area or site. In [3] authors study the stability of the model (1.1.5) by analyzing the eigenvalues of

a suitable linearization with restricted perturbations. These models track each agent by modeling the state as an $2N$ -tuple $(x_1, \dots, x_N, v_1, \dots, v_N)$ where $x_i \in \mathbb{R}^d$ and $v_i \in \mathbb{R}^d$ denoted the position and the velocity of agent i . It is not interesting to keep track of the evolution of each agent when N is very large. In this situation, it will be adequate to model by a measure on \mathbb{R}^d leading to kinetic and hydrodynamic models [9], [19]. These models are based on partial differential equations that describe the evolution of the density of the agents that formed the system. See [7], [20], [25] and reference therein. It must be noted that flocking models usually are concerned with a number of agents moving in the physical space. Newton's laws dictate that such systems have a second-order dynamics so that it is the accelerations of agents that are usually controlled. Models of first-order self-organized systems commonly arise in other applications such as opinion dynamics models or flocking situations where one may reasonably assume that agents can directly control their velocities. See [21], [31] for instance. A stochastic version of these models with multiplicative white noise are studied in [2], [17]. In [4], [25], [30] the authors study models with hierarchical leaders.

1.2 Our Contribution

In this dissertation, we provide and analyze a model which is the generalization of many existing models. Our study is based on a finite number of agents where each agent follows a similar rule, though parameters appearing in these rules may

vary from agent to agent. We further generalize the MT model in ways that are inspired by the ability to account for acceleration bounds, masking effects as well as orientation bias. We endeavor to keep the model as general and flexible as possible while ensuring flocking behavior. Moreover, despite these generalizations, we believe that many real-world phenomena may not be captured by a model that only incorporates flocking mechanisms without *steering*. Steering is defined as the additional acceleration by each agent which accounts for their individual responses to other external influences such as the need to compensate friction and gravity, pursuit of targets, and evasion of danger. In Chapter 2, we start with the MT model, discuss some of its limitations and then explore potential modifications that could provide further evidence to better understand the natural phenomena. We provide some assumptions (see Assumptions 1, 2, 3) that ensure existence and uniqueness of the derived models. Lemma 1 shows that it is vital to incorporate the steering component of each agent. In Chapter 3, we prove that the derived models flock under certain conditions. Unlike other models, our generalized model does not flock to a constant velocity. In Chapter 4 we introduce a singularly perturbed model that captures fast flocking and slow steering. Using singular perturbation theory, we derive the leading order solution which suggests flocking. More interestingly, we give an expression of the flocking velocity, see formula (4.2.7). The simulation of the model shows that the steering component of the acceleration allows the agents to follow a predefined trajectory. In Chapter 5, we observe that our model does not

prevent collision between agents. To overcome this collision problem, it is instructive to ameliorate our model. To this end, we augment the model by attractive-repulsive forces. We use Morse potential force first and then we use inter-particle bonding forces to ameliorated our model. Simulation of these models suggest that for a systematic choice of parameters, collision can be avoided.

Chapter 2: Generalization of the Model

In this chapter, we introduce a model for the dynamics of flocking and steering of a finite number of agents. In this model, each agent's acceleration consists of flocking and steering components. The flocking component is a generalization of many of the existing models and allows for the incorporation of real world features such as acceleration bounds, partial masking effects, and orientation bias. The steering component models the individual agent's own whims.

Our starting point is the model described by equations (1.1.4). That is:

$$\begin{aligned}\dot{x}_i &= v_i \\ \dot{v}_i &= \alpha(\bar{v}_i - v_i).\end{aligned}$$

We refer to this model as the MT model. We observe that the MT model has two aspects. First, the velocity alignment aspect which is given by: $\dot{v}_i = \alpha(\bar{v}_i - v_i)$ where $\alpha > 0$ is a constant and $\bar{v}_i = \sum_{j=1}^N a_{ij}v_j$ is a (time-dependent) convex combination of v_1, \dots, v_N . Regardless of the nature of this combination, in the velocity space, the acceleration of agent i is always pointed towards a point in the convex hull of all of the velocities. The second aspect of the model involves how a_{ij} depends on

the positions x_1, \dots, x_N . We note that throughout this chapter $\|z\|$ stands for the Euclidean norm of a vector $z \in \mathbb{R}^d$.

2.1 Apriori Acceleration Bounds

We start with the reasonable assumption that the magnitude of the acceleration $\|\dot{v}_i\|$ of any agent i may not exceed a certain predetermined value, say $A > 0$. It is readily observed that in the MT model (1.1.4), the acceleration of agent i is always given by $\alpha(\bar{v}_i - v_i)$ and since $\alpha > 0$ is independent of t and i , this does not readily allow for the condition $\alpha\|\bar{v}_i - v_i\| \leq A$ to be satisfied. Simply relaxing the model to allow for α to depend on i and t , readily provides for the condition on acceleration bound to be

$$\alpha_i(t) \leq \frac{A}{\|\bar{v}_i(t) - v_i(t)\|},$$

which can always be satisfied since agent i chooses a time varying value for $\alpha_i(t)$. Thus, one may regard $\alpha_i(t)$ as a scalar control input from agent i . The only condition on each agent i is that the agent accelerates in a direction parallel to $\bar{v}_i - v_i$ and pointing in the same sense so that $\alpha_i(t) > 0$. A simple feedback law that each agent i can implement may take the form

$$\alpha_i(t) = \xi_i(\bar{v}_i(t) - v_i(t)), \tag{2.1.1}$$

where $\xi_i : \mathbb{R}^d \rightarrow [0, \infty)$. Then the condition on acceleration bound becomes $\xi_i(u) \leq A/\|u\|$. Motivated by this discussion, we state the following assumption.

Assumption 1 For $i = 1, \dots, N$, the functions $\xi_i : \mathbb{R}^d \rightarrow (0, \infty)$ are C^1 (continuously differentiable), strictly positive and there exists $A > 0$ such that

$$\xi_i(u) \leq A/\|u\|, \text{ for } u \neq 0, i = 1, \dots, N. \quad (2.1.2)$$

We note that the C^1 assumption helps ensure the existence and uniqueness of solutions. A simple example of ξ_i is given by

$$\xi_i(u) = \frac{A}{\sqrt{a^2 + \|u\|^2}} \quad i = 1, \dots, N, \quad (2.1.3)$$

where $a > 0$ is some constant.

2.2 Masking Effect and Orientation Bias

In the CS model, the influence of agent j on agent i is given by the form $a_{ij} = \phi(\|x_i - x_j\|)$ whereas in the MT model it is given by

$$a_{ij} = \phi(\|x_i - x_j\|) / \sum_{k=1}^N \phi(\|x_i - x_k\|)$$

where $\phi : [0, \infty) \rightarrow [0, \infty)$. This form assumes that the influence of j on i is a function of all the pairwise distances. This specific form is not general enough to model masking effects. In order to explain this, we refer to Figure 2.1. In the position space, if a third agent l is present in the line segment joining agents i and j , then the influence of j on i may be lesser than if there were no agents present. This motivates a very general form of position dependence for a_{ij} . Additionally, the effect of agent j on agent i will depend on the orientation of the field of view of

agent i . It is natural to consider the orientation of agent i as the unit vector $v_i/\|v_i\|$. However, this is undefined when $v_i = 0$. To avoid singularities, we consider agent i 's orientation u_i to be a C^1 function of v_i , so that $u_i = \sigma_i(v_i)$ where $\sigma_i : \mathbb{R}^d \rightarrow \bar{B}^d$ where \bar{B}^d is the closed unit ball in \mathbb{R}^d . An example of σ_i is given by

$$\sigma_i(u) = \frac{u}{\sqrt{\|u\|^2 + b_i^2}}.$$

Where b_i is a nonzero real number. These two observations suggest the following form for a_{ij} :

$$a_{ij} = \phi_{ij}(x; \sigma_i(v_i)) \quad (2.2.1)$$

where $x = (x_1, \dots, x_N) \in \mathbb{R}^{Nd}$, $\sigma_i : \mathbb{R}^d \rightarrow \bar{B}^d$ and $\phi_{ij} : \mathbb{R}^{Nd} \times \mathbb{R}^d \rightarrow [0, \infty)$. We note that \bar{B}^d is the unit ball in \mathbb{R}^d . Thus the influence of agent j on agent i can be a nuanced function of the positions of all the agents as well as the velocity of agent i .

We state our assumptions on ϕ_{ij} and σ_i .

Assumption 2 For $1 \leq i, j \leq N$, $\phi_{ij} : \mathbb{R}^{Nd} \times \mathbb{R}^d \rightarrow (0, \infty)$ are C^1 and strictly positive. Moreover, ϕ_{ij} are shift invariant in position:

$$\phi_{ij}(x_1 + y, x_2 + y, \dots, x_N + y; u) = \phi_{ij}(x_1, x_2, \dots, x_N; u) \quad (2.2.2)$$

$\forall x \in \mathbb{R}^{Nd}, \forall y \in \mathbb{R}^d, \forall u \in \bar{B}^d$. Additionally, $\sigma_i : \mathbb{R}^d \rightarrow \bar{B}^d$ are C^1 .

We note that the shift invariance assumption is reasonable since the influence of agent j on agent i must only depend on the relative positions of all of the agents, but not on their absolute positions. As before, the C^1 assumption helps ensure

existence uniqueness results. The strict positivity assumptions on ϕ_{ij} are utilized in our flocking results and are a statement of the lack of complete masking. That is, each agent has a nontrivial influence on every other agent regardless of the relative configuration. Now, we provide an example of influence function with masking

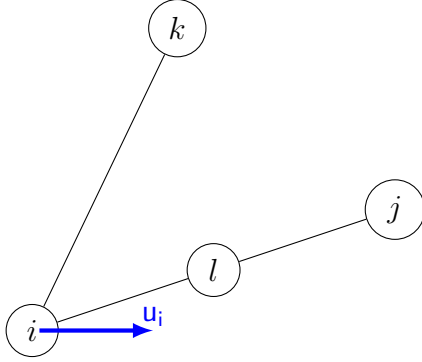


Figure 2.1: *Masking effect and orientation bias. The agents j and k are equidistant from agent i . Nevertheless, agent l contributes to the masking effect which diminishes agent j 's influence on agent i . On the other hand, agent i is moving to the right and in agent i 's field of view agent j is in a more prominent position than agent k , which diminishes agent k 's influence on agent i .*

effect. Recall that the Cucker Smale influence function is given by

$$\phi^{CS}(r_{ij}) = \frac{1}{(1 + r_{ij}^2)^\beta}.$$

Here $r_{ij} = \|x_i - x_j\|$ is the distance between agents i and agent j , and $\beta > 0$ is a parameter of the model. Before we define the influence function that takes into account the masking effect, let us first define a parameter that will tell if the masking

effect is observed. Let $r > 0$ be a positive real number. Define

$$w_{ijl} = \frac{\langle x_j - x_i, x_l - x_i \rangle}{\sqrt{\|x_j - x_i\|^2 \|x_l - x_i\|^2 + r^4}}, \quad 1 \leq i, j \leq N.$$

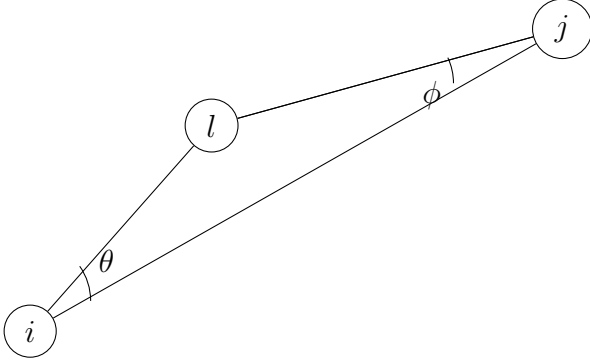


Figure 2.2: θ is the angle at i and ψ is the angle at j . This graph explains the construction of w_{ijl} .

To better explain the construction of the influence function we refer to figure (2.2). In this figure, when agent l is close to the line segment joining x_i and x_j , both angle θ and ϕ are closed to zero and masking occurs. w_{ijl} is a measure related to $\cos \theta$ and w_{jil} is the measure related to $\cos \phi$. When these angles are close to zero, w_{ijl} and w_{jil} are close to 1. We define the influence function with masking effect by:

$$\phi_{ij}^{ME}(x) = \phi^{CS}(r_{ij}) \exp \left\{ - \sum_{\substack{1 \leq l \leq N \\ l \neq i \\ l \neq j}} h(w_{ijl} + w_{jil}) \right\}. \quad (2.2.3)$$

Here, h is a positive function satisfying the following:

$$h(s) = 0 \quad \text{if } s \leq 1.9,$$

$$h(s) = 3000(s - 1.9)^3 \quad \text{if } 1.9 \leq s \leq 2.$$

The factor

$$\exp \left\{ - \sum_{\substack{1 \leq l \leq N \\ l \neq i \\ l \neq j}} h(w_{ijl} + w_{jil}) \right\}$$

takes its values between 0 and 1. Multiplying it by $\phi^{CS}(r_{ij})$ reduces the influence of agent j on agent i . The following graph depicted the effect of the multiplicative factor for the case of two agents $a_1 = (1, 0)$ and $a_2 = (2, 0)$ and the third agent is $a_3 \in [0.8, 2.2] \times [-0.5, 0.5]$.

We note that the influence function with masking effect given by (2.2.3) is symmetric, that is $\phi^{ME}(r_{ij}) = \phi^{ME}(r_{ji})$. We then define the non-symmetric influence

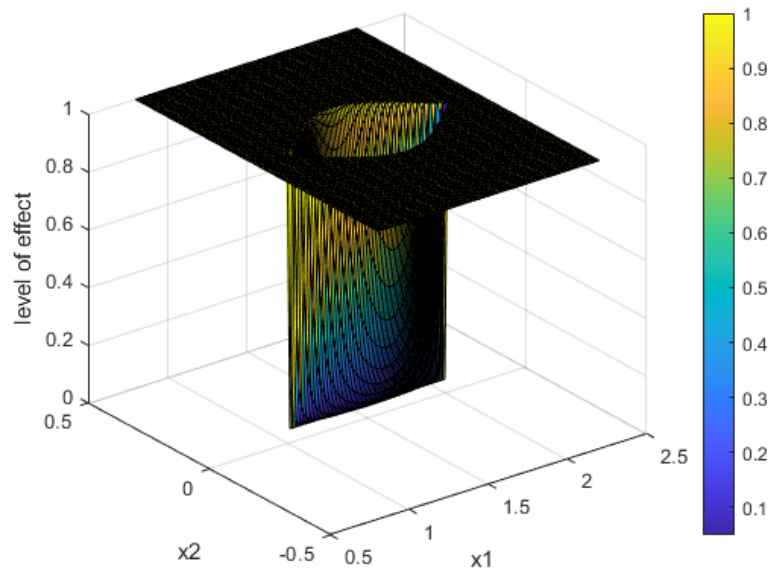


Figure 2.3: Effect of factor $\exp\{-h(w_{123} + w_{213})\}$ for two points $x_1 = (1, 0)^t$ and $x_2 = (2, 0)^t$ and the third element is in the domain $[0.8, 2.2] \times [-0.5, 0.5]$

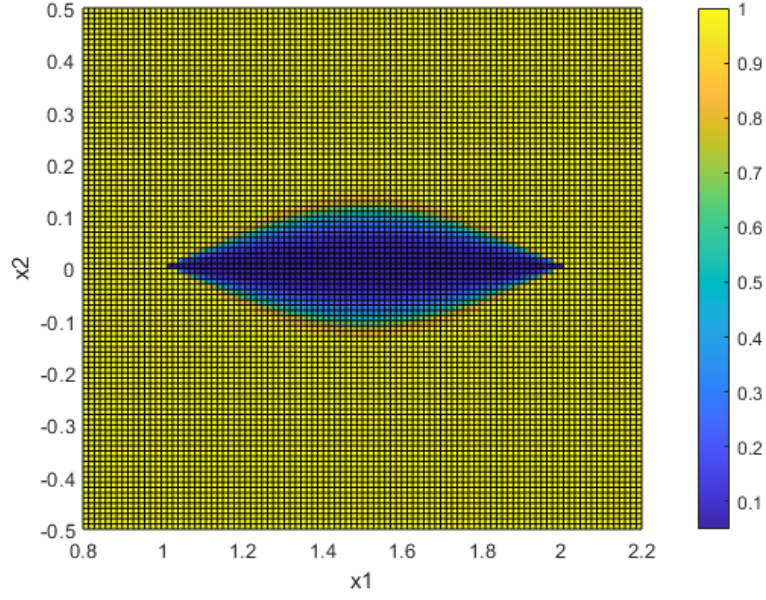


Figure 2.4: Effect of factor $\exp\{-h(w_{123} + w_{213})\}$ for two points $x_1 = (1, 0)^t$ and $x_2 = (2, 0)^t$ and the third element is in the domain $[0.8, 2.2] \times [-0.5, 0.5]$ see from above

function that takes into account the masking effect by:

$$\phi_{ij}(x) = \frac{\phi_{ij}^{ME}(x)}{\sum_{k=1}^N \phi_{ik}^{ME}(x)}.$$

2.3 The Open Loop and Closed Loop Models

It is instructive to consider our general model as forming two layers. The first layer is the “open loop” model given by

$$\begin{aligned}
 \dot{x}_i &= v_i, \\
 \dot{v}_i &= \alpha_i(\bar{v}_i - v_i), \\
 \bar{v}_i &= \sum_{j=1}^N a_{ij}v_j, \\
 a_{ij} &\geq 0, \quad \sum_{j=1}^N a_{ij} = 1, \quad \alpha_i \geq 0
 \end{aligned} \tag{2.3.1}$$

where α_i and a_{ij} are considered to be given functions of t , which can be regarded as control inputs from agent i . The second layer of our model specifies how α_i and a_{ij} are chosen as functions of positions and velocities, thus “closing the loop”. The closed loop model thus contains the equations

$$\begin{aligned}
 \dot{x}_i &= v_i \\
 \dot{v}_i &= \alpha_i(\bar{v}_i - v_i) \\
 \bar{v}_i &= \sum_{j=1}^N \phi_{ij}(x; u_i)v_j \\
 u_i &= \sigma_i(v_i) \\
 \alpha_i &= \xi_i(\bar{v}_i - v_i)
 \end{aligned} \tag{2.3.2}$$

for $i = 1, \dots, N$, where ξ_i and ϕ_{ij} satisfy Assumptions 1 and 2 respectively.

2.4 Inclusion of Friction

In the real physical world, forces such as aerodynamic friction are present. We will consider a form of friction which is proportional to some power of the velocity. We have the following (open loop) system:

$$\begin{aligned}\dot{x}_i &= v_i \\ \dot{v}_i &= \alpha_i(t)(\bar{v}_i - v_i) - c_i \|v_i\|^r v_i,\end{aligned}\tag{2.4.1}$$

where $r \geq 0$. The following lemma shows very trivial asymptotic behavior.

Lemma 1 *Suppose $\{x_i(t), v_i(t)\}_{i=1}^N$ is a C^1 solution of the system (2.4.1). Then for each i*

$$\lim_{t \rightarrow \infty} v_i(t) = 0.$$

Remark 1 *We note that the Lemmas 5 and 7 given in the appendix will be frequently used in the proofs of the results in this thesis.*

Proof We define an energy of the system by $E = \max_{1 \leq j \leq N} E_j$ where $E_j = \frac{1}{2} \|v_j\|^2$.

Then by Lemmas 5 and 7 $E(t)$ is absolutely continuous and $\frac{dE}{dt}(t) = \frac{dE_i}{dt}(t)$ for almost all t where $i = i(t)$ is an index of the maximum. Thus, for almost all t ,

$$\begin{aligned}\frac{dE}{dt} &= \langle v_i, \dot{v}_i \rangle = \langle v_i, \alpha_i(\bar{v}_i - v_i) - c_i \|v_i\|^r v_i \rangle = -c_i \|v_i\|^{r+2} + \alpha_i \langle \bar{v}_i, v_i \rangle - \alpha_i \|v_i\|^2 \\ &= -c_i \|v_i\|^{r+2} + \alpha_i \sum_j a_{ij} \langle v_i, v_j \rangle - \alpha_i \|v_i\|^2 \\ &\leq -c_i \|v_i\|^{r+2} - \alpha_i \|v_i\|^2 + \alpha_i \|v_i\| \sum_j a_{ij} \|v_j\| \leq -c_i \|v_i\|^{r+2}\end{aligned}$$

where we have used the Cauchy-Schwartz inequality and the fact that $\|v_i\| \geq \|v_j\|$ for all j . We also note that the index i in general varies with t . Letting $\underline{c} = \min_i c_i$, we have

$$\frac{dE(t)}{dt} \leq -\underline{c}\|v_i\|^{r+2} \leq -2^{\frac{r}{2}+1} \underline{c} (E(t))^{\frac{r}{2}+1}. \quad (2.4.2)$$

Multiplying both sides by $(E(t))^{-\frac{r}{2}-1}$, we have

$$\begin{aligned} (E(t))^{-\frac{r}{2}-1} \frac{dE(t)}{dt} &\leq -2^{\frac{r}{2}+1} \underline{c} \\ -\frac{2}{r} \frac{dE(t)^{-\frac{r}{2}}}{dt} &\leq -2^{\frac{r}{2}+1} \underline{c} \end{aligned}$$

integrating the last inequality from 0 to t after some algebra manipulation, we have

$$(E(t))^{-\frac{r}{2}} - (E(0))^{-\frac{r}{2}} \geq 2^{\frac{r}{2}} r \underline{c} t$$

which implies that

$$E(t) \leq \frac{1}{((E(0))^{-\frac{r}{2}} + 2^{\frac{r}{2}} r \underline{c} t)^{\frac{2}{r}}}.$$

Thus $E(t) \rightarrow 0$ as $t \rightarrow \infty$. ■

2.5 Ring Mill Phenomena

In nature, many collective motions of living species can exhibit milling phenomena. That is a phenomenon in which agents rotate about an axis of rotation with a constant angular velocity. It is instructive to check if our model so far can have a milling solution. For sake of simplicity, we will assume that agents are in \mathbb{R}^3

and that the axis of rotation is the z -axis. So, for agent i ,

$$\begin{aligned} x_i &= R_i \cos(\omega_i t + \theta_i) e_1 + R_i \sin(\omega_i t + \theta_i) e_2 + k_i e_3 \\ v_i = \dot{x}_i &= -R_i \omega_i \sin(\omega_i t + \theta_i) e_1 + R_i \omega_i \cos(\omega_i t + \theta_i) e_2 \\ \dot{v}_i = \ddot{x}_i &= -R_i \omega_i^2 \cos(\omega_i t + \theta_i) e_1 - R_i \omega_i^2 \sin(\omega_i t + \theta_i) e_2 \\ &= -\omega_i^2 (x_i - k_i e_3). \end{aligned}$$

We have that, v_i and $(x_i - k_i e_3)$ are perpendicular. This implies that

$$\langle \dot{v}_i, v_i \rangle = \langle \bar{v}_i - v_i, v_i \rangle = 0$$

We then deduce that:

$$\langle \bar{v}_i, v_i \rangle = \|v_i\|^2 \quad (2.5.1)$$

Let us show that

$$\|v_i\| = \|v_j\| \quad \forall i, j \in \{1, \dots, N\}. \quad (2.5.2)$$

From (2.5.1) and Cauchy Schwartz inequality, we have

$$\begin{aligned} \|v_i\|^2 &= \sum_{j=1}^N a_{ij} \langle v_i, v_j \rangle \leq \sum_{j=1}^N a_{ij} \|v_i\| \|v_j\| \\ \|v_i\| &\leq \sum_{j=1}^N a_{ij} \|v_j\|. \end{aligned}$$

Choose i such that $\|v_i\| = \max \|v_j\|$. Suppose that there exists k such that $\|v_k\| < \|v_i\|$. Then

$$\|v_i\| \leq \sum_{j=1}^N a_{ij} \|v_j\| < \sum_{j=1}^N a_{ij} \|v_i\| = \|v_i\|.$$

This implies that $\|v_i\| < \|v_i\|$. It follows that $\|v_i\| = \|v_j\|$ for all $i, j \in \{1, \dots, N\}$

Now let us show that

$$\bar{v}_i = v_i \quad \forall i \in \{1, \dots, N\}. \quad (2.5.3)$$

From (2.5.1),

$$\langle \bar{v}_i, v_i \rangle = \|v_i\|^2$$

Using Cauchy Schwartz Inequality, we have

$$\|\bar{v}_i\| \|v_i\| \geq \|v_i\|^2$$

That is $\|\bar{v}_i\| \geq \|v_i\|$

By definition, $\bar{v}_i = \sum_j a_{ij} v_j$. We have:

$$\|\bar{v}_i\| \leq \sum_j a_{ij} \|v_j\| \leq \left(\sum_j a_{ij} \right) \|v_i\| \leq \|v_i\|$$

We have used the triangle inequality and (2.5.2) It comes that $\|\bar{v}_i\| = \|v_i\|$

Hence,

$$\langle \bar{v}_i, v_i \rangle = \|v_i\|^2 = \|\bar{v}_i\| \|v_i\|.$$

This shows that $\bar{v}_i = v_i$.

The acceleration of agent i becomes

$$\dot{v}_i = \alpha_i (\bar{v}_i - v_i) = 0.$$

That is

$$\dot{v}_i = \ddot{x}_i = -\omega_i^2 (x_i - k_i e_3) = 0$$

This implies that

$$\omega_i = 0 \text{ or } x_i = k_i e_3$$

In either case, $v_i = 0$. Thus all the agents are stationary. We conclude that our model so far does not have a milling solution.

The addition of the friction shows that the asymptotic velocities go to zero. Also, the model does not have a ring mill solution. These observations and other real world considerations show that in addition to pure flocking, there should be a “steering” component to each agent’s acceleration to model its own impulse.

2.6 Steering

In reality, a group of agents may want to follow a desired trajectory in addition to staying together as a flock. This necessitates an extra “steering” term. Thus, each agent i may have an extra acceleration $\beta_i(t)$ which contributes to steering. This steering term can also act to cancel other external forces such as friction and gravity. We interpret $\beta_i(t)$ in the following as the steering component in excess of friction and gravity.

This leads to the system

$$\begin{aligned}
\dot{x}_i &= v_i, \\
\dot{v}_i &= \alpha_i(\bar{v}_i - v_i) + \beta_i, \\
\bar{v}_i &= \sum_{j=1}^N a_{ij} v_j, \\
a_{ij} &\geq 0, \quad \sum_{j=1}^N a_{ij} = 1, \quad \alpha_i \geq 0
\end{aligned} \tag{2.6.1}$$

for the open loop with steering and

$$\begin{aligned}
\dot{x}_i &= v_i \\
\dot{v}_i &= \alpha_i(\bar{v}_i - v_i) + \beta_i \\
\bar{v}_i &= \sum_{j=1}^N \phi_{ij}(x; u_i) v_j \\
u_i &= \sigma_i(v_i) \\
\alpha_i &= \xi_i(\bar{v}_i - v_i)
\end{aligned} \tag{2.6.2}$$

for the closed loop with steering.

Assumption 3 *The steering functions $\beta_i : [0, \infty) \rightarrow \mathbb{R}^d$ for $i = 1, \dots, N$ are continuous.*

2.7 Existence and Uniqueness

We briefly discuss existence and uniqueness of solutions of the open loop and closed loop models (2.6.1) and (2.6.2). The open loop model is linear and non-autonomous and hence it is adequate to assume that $\alpha_i(t)$, $a_{ij}(t)$ and $\beta_i(t)$ are all

continuous in time. The closed loop model is of the form

$$\dot{z} = F(z) + \beta(t)$$

where $z = (x_1, \dots, x_N, v_1, \dots, v_N) \in \mathbb{R}^{2Nd}$ and F is C^1 by our assumptions on ϕ_{ij} and ξ_i . Again if we assume $\beta_i(t)$ to be continuous in t then for any given initial condition for $z(0)$, we are assured of a unique solution in an open maximal interval of time containing 0.

In order to discuss flocking behavior, it is important to ensure that the forward maximal interval of existence is $[0, \infty)$. When the steering is open-loop with Assumption 3 it is shown in Lemma 8 that the forward maximal interval is infinite. When steering is considered to be closed-loop, that is some function of position and velocity, then we use Lemmas 8 and 9.

Chapter 3: Analysis of the Model

The main objective in this chapter is to analyze the model derived in Chapter 2. We start the chapter by providing some definitions and some lemmas that will help for the analysis of the model. We then state and prove Theorem 1 which is the generalization of the main theorem in [25].

3.1 Preliminaries

Definition 1 *Let $\{x_i(t), v_i(t)\}$ $i = 1, \dots, N$ be a given system, and let $d_X(t)$ and $d_V(t)$ denote its diameters in position and velocity spaces \mathbb{R}^{Nd} ,*

$$d_X(t) = \max_{i,j} \|x_j(t) - x_i(t)\| \quad (3.1.1a)$$

$$d_V(t) = \max_{i,j} \|v_j(t) - v_i(t)\|. \quad (3.1.1b)$$

Definition 2 *The system $\{x_i(t), v_i(t)\}$ $i = 1, \dots, N$ is said to converge to a flock if the following two conditions hold,*

$$\sup_{t \geq 0} d_X(t) < \infty \quad (3.1.2a)$$

$$\lim_{t \rightarrow \infty} d_V(t) = 0. \quad (3.1.2b)$$

The method that we are using in this chapter is based in the notion of active set.

The reader who is interested for more details of the following may refer to [25].

Definition 3 *Active sets*

Let $A = \{a_{ij}\}$ be a normalized influence matrix, $a_{ij} \geq 0$, $\sum_{j=1}^N a_{ij} = 1$. Fix $\theta > 0$.

The active set , $\Lambda_p(\theta)$ is the set of agents which influence 'p' more than θ

$$\Lambda_p(\theta) = \{j | a_{pj} \geq \theta\}$$

The global active set, $\Lambda(\theta)$, is the intersection of all the active sets at that level,

$$\Lambda(\theta) = \bigcap_p \Lambda_p(\theta)$$

Lemma 2 [25]

Let S be and anti-symmetric matrix, $S_{ij} = -S_{ji}$ with maximal entry $|S_{ij}| \leq M$.

Let $u, w \in \mathbb{R}^n$ be two given vectors with positive entries, $u_i, w_i \geq 0$, and let \bar{U}, \bar{W} denoted their respective sum, $\bar{U} = \sum_i u_i$ and $\bar{W} = \sum_j w_j$. Fix $\theta > 0$ and let $\lambda(\theta)$ denoted the number of “active entries” of u and w at the level θ , in sense that,

$$\lambda(\theta) = |\Lambda(\theta)|$$

$$\Lambda(\theta) = \{j | u_j \geq \theta \bar{U} \text{ and } w_j \geq \theta \bar{W}\}.$$

Then for every $\theta > 0$, we have

$$|\langle Su, w \rangle| \leq M \bar{U} \bar{W} (1 - \lambda^2(\theta) \theta^2).$$

Proof Please refer to [25]. ■

Lemma 3 *Let $\{v_i\}_{i=1}^N$ be a set of vectors in \mathbb{R}^d and let Ω be their convex hull. If v_p and v_q delimit the diameter of the convex hull, (that is v_p and v_q are furthest apart), then for each $v \in \Omega$*

$$\langle v_p - v_q, v - v_q \rangle \geq 0.$$

Proof Let the diameter of Ω equal $\|v_p - v_q\|$. We first show that

$$\langle v_p - v_q, v_i - v_q \rangle \geq 0 \quad \forall i.$$

Let H_{pq} be the hyperplane passing through v_q and is perpendicular to $v_p - v_q$. (See Figure 3.1). Suppose there is some i such that $\langle v_p - v_q, v_i - v_q \rangle < 0$. This shows that v_i and v_p will be on opposite sides of the hyper plane H_{pq} , implying that $\|v_i - v_p\| > \|v_q - v_p\|$, a contradiction. Given any $v \in \Omega$, there exist $a_i \geq 0$ for $i = 1, \dots, n$ such that $\sum_{i=1}^N a_i = 1$ and $v = \sum_{j=1}^N a_j v_j$. Hence

$$\langle v_p - v_q, v - v_q \rangle = \langle v_p - v_q, \sum_{i=1}^N a_i (v_i - v_q) \rangle \geq 0.$$
■

3.2 Analysis of the Open Loop

We shall suppose that Assumptions 1, 2, and 3 hold. We have the following theorem:

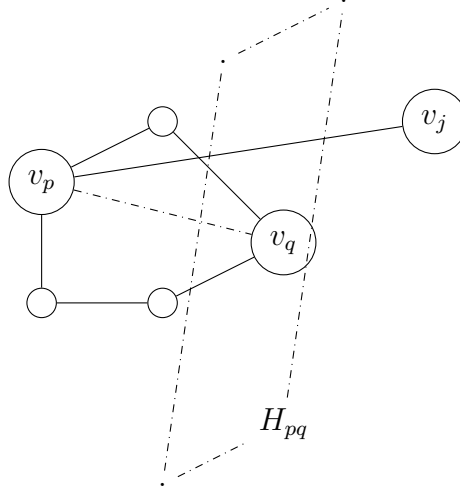


Figure 3.1: *Illustration of the lemma*

Theorem 1 *Let $(x(t), v(t)) \in \mathbb{R}^{Nd} \times \mathbb{R}^{Nd}$ be a C^1 solution of the open loop (2.6.1). At time t , let $d_V(t) = \|v_p(t) - v_q(t)\|$. Fix an arbitrary $\theta > 0$ and let $\lambda_{pq}(\theta)$ be the number of agents in the common active set $\Lambda_{pq}(\theta)$ associated with the influence matrix $a_{ij}(t)$ of the system. Let $\alpha_0(t) = \min_i \alpha_i(t)$. Then for almost all t , the diameters of the system, $d_X(t)$, $d_V(t)$ and $d_\beta(t)$ satisfy :*

$$\begin{aligned} \frac{d}{dt} d_X(t) &\leq d_V(t) \\ \frac{d}{dt} d_V(t) &\leq -\alpha_0 \lambda_{pq}^2(\theta) \theta^2 d_V(t) + d_\beta(t). \end{aligned} \tag{3.2.1}$$

Remark 2 *In Theorem (1), we note that p and q are functions of t , and so is $\lambda_{pq}(\theta)$. This theorem is a generalization of Theorem 3.4 of [25] where $\alpha_i(t)$ was independent of i and t . One needs Lemma 3 to handle the extra terms that appear in our analysis.*

Proof By Lemma 5, $d_X(t)$ is absolutely continuous. We choose $i = i(t)$ and

$j = j(t)$ such that $d_X(t) = \|x_i(t) - x_j(t)\|$ for all t . Using Lemma 7 we obtain

$$\left| \frac{d}{dt}(d_X(t))^2 \right| = \left| \frac{d}{dt}\|x_i - x_j\|^2 \right| = 2|\langle x_i - x_j, v_i - v_j \rangle|.$$

Hence

$$\left| 2\|x_i - x_j\| \frac{d}{dt}\|x_i - x_j\| \right| = 2|\langle x_i - x_j, v_i - v_j \rangle| \leq 2\|x_i - x_j\|\|v_i - v_j\|.$$

This yields that for almost all t

$$\frac{d}{dt}d_X(t) \leq \|v_i - v_j\| \leq d_V(t).$$

Note that if for some $t > 0$, $d_X(t) = 0$ and $d_X(t)$ is differentiable, then $\frac{d}{dt}d_X(t) = 0$.

For the second inequality, we again proceed by using Lemmas 5 and 7. Let $p = p(t)$ and $q = q(t)$ be such that $d_V(t) = \|v_p - v_q\|$ for all t . Then (for almost all t)

$$\begin{aligned} \frac{d}{dt}(d_V(t))^2 &= \frac{d}{dt}(\|v_p - v_q\|^2) = 2\langle v_p - v_q, \dot{v}_p - \dot{v}_q \rangle \\ &= 2\langle v_p - v_q, \alpha_p(\bar{v}_p - v_p) - \alpha_q(\bar{v}_q - v_q) \rangle + 2\langle v_p - v_q, \beta_p - \beta_q \rangle \\ &= 2\alpha_p\langle v_p - v_q, \bar{v}_p - v_p \rangle - 2\alpha_q\langle v_p - v_q, \bar{v}_q - v_q \rangle + 2\langle v_p - v_q, \beta_p - \beta_q \rangle. \end{aligned}$$

We proceed by assuming WLOG that $\alpha_p \leq \alpha_q$ and write

$$\begin{aligned} \frac{d}{dt}(\|v_p - v_q\|^2) &= 2\alpha_p\langle v_p - v_q, \bar{v}_p - \bar{v}_q \rangle - 2\alpha_p\|v_p - v_q\|^2 \\ &\quad - 2(\alpha_q - \alpha_p)\langle v_p - v_q, \bar{v}_q - v_q \rangle + 2\langle v_p - v_q, \beta_p - \beta_q \rangle. \end{aligned}$$

Using Lemma (3), Cauchy-Schwartz inequality and the fact that $\|\beta_p - \beta_q\| \leq d_\beta$, we have:

$$\frac{d}{dt}(\|v_p - v_q\|^2) \leq 2\alpha_p\langle v_p - v_q, \bar{v}_p - \bar{v}_q \rangle - 2\alpha_p\|v_p - v_q\|^2 + 2\|v_p - v_q\|d_\beta.$$

Moreover

$$\begin{aligned}\bar{v}_p - \bar{v}_q &= \sum_{j=1}^N a_{pj} v_j - \bar{v}_q = \sum_{j=1}^N a_{pj} (v_j - \bar{v}_q) \\ &= \sum_{j=1}^N a_{pj} (v_j - \sum_{i=1}^N a_{qi} v_i) = \sum_{i,j}^N a_{pj} a_{qi} (v_j - v_i).\end{aligned}$$

Hence

$$\frac{d}{dt}(\|v_p - v_q\|^2) \leq 2\alpha_p \sum_{i,j}^N a_{pj} a_{qi} \langle v_p - v_q, v_j - v_i \rangle - 2\alpha_p \|v_p - v_q\|^2 + 2d_\beta \|v_p - v_q\|.$$

Now we use Lemma (2) with $u_i = a_{pi}$, $w_i = a_{qi}$, and the anti-symmetric matrix

$$S_{ij} = \langle v_p - v_q, v_i - v_j \rangle.$$

Since $|S_{ij}| \leq d_V^2$, we have

$$\left| \sum_{i,j}^N a_{pj} a_{qi} \langle v_p - v_q, v_j - v_i \rangle \right| \leq d_V^2 (1 - \lambda_{pq}^2(\theta) \theta^2)$$

Therefore we have

$$\frac{d}{dt}(\|v_p - v_q\|^2) \leq 2\alpha_p d_V^2 (1 - \lambda_{pq}^2(\theta) \theta^2) - 2\alpha_p \|v_p - v_q\|^2 + 2d_\beta \|v_p - v_q\|$$

Noting that v_p and v_q are such that $\|v_p(t) - v_q(t)\| = d_V(t)$ and that $\alpha_p(t) \geq \alpha_0(t)$

by definition, we have

$$\frac{d}{dt}(d_V(t)^2) \leq -2\alpha_0 d_V^2 \lambda_{pq}^2(\theta) \theta^2 + 2d_\beta d_V.$$

An argument similar to the one used in deriving the first inequality proves the second inequality. Theorem (1) is then proved. ■

The following corollary is immediate.

Corollary 1 *If $\lambda(\theta)$ is the number of elements in the global active set $\Lambda(\theta)$ and if $\underline{\alpha}$ denotes the infimum of $\alpha_i(t)$ over i and $t \geq 0$ then*

$$\frac{d}{dt}d_X(t) \leq d_V(t). \quad (3.2.2a)$$

$$\frac{d}{dt}d_V(t) \leq -\underline{\alpha}\lambda(\theta)\theta^2 d_V(t) + d_\beta(t). \quad (3.2.2b)$$

3.3 Analysis of the Closed Loop

As observed in Section 2.7, Assumptions 1, 2 and 3 guarantee existence and uniqueness of a solution to the closed-loop equations on the time interval $[0, \infty)$. Moreover, this solution is C^1 in time t . We note that, if all steering terms β_i are equal for all t , then $d_\beta(t) = 0$ and the system of inequalities given by (3.2.2a) and (3.2.2b) show that the diameter d_V is decreasing in time. Even in this case, in order to show flocking, one needs stronger inequalities. To that end, we shall modify the ideas from Ha et al [18] and also from Motsch and Tadmor [25] in order to prove the flocking results.

We define the function $\psi : [0, \infty) \rightarrow (0, \infty)$ by

$$\psi(r) = \min_{1 \leq i, j \leq N} \min\{\phi_{ij}(x; u) \mid \|x_l - x_k\| \leq r, u \in \bar{B}^d \text{ and } 1 \leq l, k \leq N\}. \quad (3.3.1)$$

In order to see that the minimum exists, we observe that by shift invariance (Assumption 2),

$$\begin{aligned} & \{\phi_{ij}(x; u) \mid \|x_l - x_k\| \leq r, u \in \bar{B}^d\} \\ &= \{\phi_{ij}(x; u) \mid x_1 = 0, \|x_l - x_k\| \leq r, u \in \bar{B}^d\} \end{aligned}$$

and that

$$\{(x, u) \in \mathbb{R}^{Nd} \times \bar{B}^d \mid x_1 = 0, \|x_l - x_k\| \leq r, u \in \bar{B}^d\}$$

is a compact set and that ϕ_{ij} are continuous. Since ϕ_{ij} are strictly positive by Assumption 2, it follows that ψ is strictly positive. Moreover, it is also clear that ψ is a decreasing (non-increasing) function. Since ψ is decreasing, it is also positive and measurable, and hence $\int_0^{r_0} \psi(r) dr < \infty$ and $\int_0^\infty \psi(r) dr \leq \infty$ are well-defined.

Lemma 4 *Let $\underline{\alpha}$ be the infimum of $\alpha_i(t)$ over i and $t \geq 0$. Suppose that*

$$\int_0^\infty d_\beta(t) dt < \infty.$$

Then $\underline{\alpha} > 0$.

Proof Let M be defined by

$$M = d_V(0) + \int_0^\infty d_\beta(t) dt.$$

Then from (3.2.2b) it follows that $d_V(t) \leq M$ for all $t \geq 0$. Hence, for all $t \geq 0$ and for all $1 \leq i \leq N$, $\|\bar{v}_i(t) - v_i(t)\| \leq d_V(t) \leq M$, where we have used the fact that \bar{v}_i is in the convex hull of all velocities v_j . Now

$$\begin{aligned} \underline{\alpha} &= \inf\{ \xi_i(\bar{v}_i(t) - v_i(t)) \mid t \geq 0, 1 \leq i \leq N \}, \\ &\geq \min\{ \xi_i(u) \mid 0 \leq \|u\| \leq M, 1 \leq i \leq N \} > 0, \end{aligned}$$

where we have used the fact that ξ_i are continuous by Assumption 1. ■

Theorem 2 Consider the closed loop system (2.6.2). Suppose ψ is defined by (3.3.1)

and that

$$\int_0^\infty d_\beta(t) dt < \infty \quad \text{and} \quad \lim_{t \rightarrow \infty} d_\beta(t) = 0.$$

Further suppose that the initial diameters satisfy

$$d_V(0) + \int_0^\infty d_\beta(t) dt < \underline{\alpha} N^2 \int_{d_X(0)}^\infty \psi(s) ds. \quad (3.3.2)$$

Then the solution $(x(t), v(t))$ flocks. In particular, if $\int_0^\infty \psi(s) ds = \infty$, then the condition on initial diameters is always satisfied.

Proof At any given time, by choosing $\theta(t) = \sqrt{\psi(d_X(t))}$, one readily obtains that the number of elements in the global active set is N , and hence the inequality

$$\frac{d}{dt} d_V(t) \leq -\underline{\alpha} N^2 \psi(d_X(t)) d_V(t) + d_\beta(t). \quad (3.3.3)$$

We define the energy functional $\mathcal{E} : \mathbb{R}^{Nd} \times \mathbb{R}^{Nd} \rightarrow \mathbb{R}$

$$\mathcal{E}(d_X(t), d_V(t)) = d_V(t) + \underline{\alpha} N^2 \int_0^{d_X(t)} \psi(s) ds, \quad (3.3.4)$$

The time derivative of the energy functional satisfies

$$\dot{\mathcal{E}} = \dot{d}_V + \underline{\alpha} N^2 d_V \psi(d_X) \leq d_\beta.$$

Hence

$$\mathcal{E}(d_V(t), d_X(t)) - \mathcal{E}(d_V(0), d_X(0)) \leq \int_0^t d_\beta(s) ds,$$

Which implies that

$$d_V(t) - d_V(0) \leq -\underline{\alpha} N^2 \int_0^{d_X(t)} \psi(s) ds + \underline{\alpha} N^2 \int_0^{d_X(0)} \psi(s) ds + \int_0^t d_\beta(s) ds.$$

We deduce that

$$d_V(t) - d_V(0) \leq \underline{\alpha} N^2 \int_{d_X(t)}^{d_X(0)} \psi(s) ds + \int_0^t d_\beta(s) ds. \quad (3.3.5)$$

By the assumption (3.3.2), there exists d_* (independent of t) such that

$$\int_0^\infty d_\beta(t) dt + d_V(0) \leq \underline{\alpha} N^2 \int_{d_X(0)}^{d_*} \psi(s) ds. \quad (3.3.6)$$

Replacing this inequality in (3.3.5), we obtain that

$$d_V(t) \leq \underline{\alpha} N^2 \int_{d_X(t)}^{d_X(0)} \psi(s) ds + \underline{\alpha} N^2 \int_{d_X(0)}^{d_*} \psi(s) ds \leq \underline{\alpha} N^2 \int_{d_X(t)}^{d_*} \psi(s) ds.$$

Since $d_V(t) \geq 0$, we have that the diameter in the position space is uniformly bounded. That is, $d_X(t) \leq d_*$ for all $t \geq 0$. Defining $\psi_* = \psi(d_*)$, we note that $\psi(s) \geq \psi_*$ for $s \in [0, d_*]$. Using the inequality

$$\frac{d}{dt} d_V(t) \leq -\underline{\alpha} N^2 \psi(d_X(t)) d_V + d_\beta,$$

we have that

$$\frac{d}{dt} d_V(t) \leq -\underline{\alpha} N^2 \psi_* d_V + d_\beta.$$

Which implies that:

$$d_V(t) \leq e^{-\underline{\alpha} N^2 \psi_* t} d_V(0) + \int_0^t e^{-\underline{\alpha} N^2 \psi_* (t-s)} d_\beta(s) ds$$

Now let us show that the velocity diameter goes to zero asymptotically. The first term above goes to zero asymptotically in time. The second term can be written as

$$\frac{\int_0^t e^{\underline{\alpha} N^2 \psi_* s} d_\beta(s) ds}{e^{\underline{\alpha} N^2 \psi_* t}}.$$

There are two cases. If

$$\lim_{t \rightarrow \infty} \int_0^t e^{\alpha N^2 \psi_* s} d_\beta(s) ds < \infty$$

then this second term clearly limits to zero. On the other hand, the limit above is infinity and hence an application of L'Hospital's rule and the hypothesis that $\lim_{t \rightarrow \infty} d_\beta(t) = 0$ shows that

$$\lim_{t \rightarrow \infty} \frac{\int_0^t e^{\alpha N^2 \psi_* s} d_\beta(s) ds}{e^{\alpha N^2 \psi_* t}} = \lim_{t \rightarrow \infty} \frac{e^{\alpha N^2 \psi_* t} d_\beta(t)}{e^{\alpha N^2 \psi_* t}} = \lim_{t \rightarrow \infty} d_\beta(t) = 0.$$

■

Remark 3 *It comes that our generalized model of flocking with steering flocks under some initial conditions. Unlike the case of many existing model, the velocities are not necessarily in the convex hull of initial velocities. Also, we did not prove that this asymptotic velocity is a constant.*

Chapter 4: Fast Flocking with Slow Steering

We consider the model given by (2.6.2) and investigate the scenario where flocking is much faster than steering. In the singular perturbation approach, we capture this by the introduction of a small parameter ϵ . For ease of analysis, we ignore the orientation bias and assume that $a_{ij} = \phi_{ij}(x)$. This leads us to the family of equations

$$\begin{aligned}
 \dot{x}_i &= v_i \\
 \dot{v}_i &= \frac{\alpha_i}{\epsilon}(\bar{v}_i - v_i) + \beta_i \\
 \bar{v}_i &= \sum_{j=1}^N \phi_{ij}(x) v_j \\
 \alpha_i &= \xi_i(\bar{v}_i - v_i) \quad \forall i = 1, \dots, N.
 \end{aligned} \tag{4.0.1}$$

Here, $0 < \epsilon \ll 1$ is a parameter that allows the model to flock rapidly.

Let $x_i(t, \epsilon)$ and $v_i(t, \epsilon)$ for all $i = 1, \dots, N$ be the solution of our new model (4.0.1). We expand these solutions and some related variables of the model in a

power series in ϵ :

$$\begin{aligned}
x_i(t, \epsilon) &= x_{i,0}(t) + \epsilon x_{i,1}(t) + \dots \\
v_i(t, \epsilon) &= v_{i,0}(t) + \epsilon v_{i,1}(t) + \dots \\
\alpha_i(t, \epsilon) &= \alpha_{i,0}(t) + \epsilon \alpha_{i,1}(t) + \dots \\
\bar{v}_i(t, \epsilon) &= \bar{v}_{i,0}(t) + \epsilon \bar{v}_{i,1}(t) + \dots \\
\beta_i(t, \epsilon) &= \beta_{i,0}(t) + \epsilon \beta_{i,1}(t) + \dots
\end{aligned} \tag{4.0.2}$$

4.1 Leading Order Behavior

We shall use $x_0(t)$ to denote $(x_{1,0}(t), \dots, x_{N,0}(t))$, and likewise $v_0(t)$ and $\beta_0(t)$.

We are interested in characterizing the leading order terms $x_0(t)$ and $v_0(t)$. We note that x_i^k and v_i^k are the k th components of the i th agent's position and velocity. Also $x_{i,0}^k$ and $x_{i,1}^k$ denote the leading order and the next order terms of x_i^k and likewise for $v_{i,0}^k$ and $v_{i,1}^k$. In what follows, we frequently omit showing the dependence on time for brevity. Substituting the expansions (4.0.2) into (4.0.1) we obtain

$$\begin{aligned}
\dot{x}_{i,0} + \epsilon \dot{x}_{i,1} + \dots &= v_{i,0} + \epsilon v_{i,1} + \dots \\
\dot{v}_{i,0} + \epsilon \dot{v}_{i,1} + \dots &= \frac{1}{\epsilon} (\alpha_{i,0} + \epsilon \alpha_{i,1} + \dots) (\bar{v}_{i,0} - v_{i,0}) \\
&\quad + \epsilon (\bar{v}_{i,1} - v_{i,1}) + \dots + \beta_{i,0}(t) + \epsilon \beta_{i,1}(t) + \dots
\end{aligned} \tag{4.1.1}$$

Result 1 *The leading order and the next order terms of \bar{v}_i are:*

$$\begin{aligned}
\bar{v}_{i,0} &= \sum_{j=1}^N \phi_{ij}(x_0) v_{j,0} \\
\bar{v}_{i,1} &= \sum_{j=1}^N \phi_{ij}(x_0) v_{j,1} + \sum_{j=1}^N \left\{ \sum_{l=1}^N \sum_{k=1}^d \frac{\partial \phi_{ij}}{\partial x_l^k}(x_0) x_{l,1}^k \right\} v_{j,0}.
\end{aligned} \tag{4.1.2}$$

Proof Using Taylor's expansion on ϕ_{ij} ,

$$\begin{aligned}\phi_{ij}(x)v_j &= \phi_{ij}(x_{1,0} + \epsilon x_{1,1}, \dots, x_{N,0} + \epsilon x_{N,1})(v_{j,0} + \epsilon v_{j,1} + \dots) \\ &= \left(\phi_{ij}(x_0) + \epsilon \sum_{l=1}^N \sum_{k=1}^d \frac{\partial \phi_{ij}(x_0)}{\partial x_l^k} x_{l,1}^k + \dots \right) (v_{j,0} + \epsilon v_{j,1} + \dots) \\ &= \phi_{ij}(x_0)v_{j,0} + \epsilon \left(\phi_{ij}(x_0) + \sum_{l=1}^N \sum_{k=1}^d \frac{\partial \phi_{ij}(x_0)}{\partial x_l^k} x_{l,1}^k \right) v_{j,0} + \dots\end{aligned}$$

then taking the sum from 0 to N on both sides, we have

$$\bar{v}_j = \sum_{j=1}^N \phi_{ij}(x_0)v_{j,0} + \epsilon \sum_{j=1}^N \left(\phi_{ij}(x_0)v_{j,1} + \left\{ \sum_{l=1}^N \sum_{k=1}^d \frac{\partial \phi_{ij}(x_0)}{\partial x_l^k} x_{l,1}^k \right\} v_{j,0} \right) + \dots$$

This proves our result. ■

We then have the following theorem describing the leading order approximation.

Result 2 *The leading order $x_0(t)$ of our model flocks. Furthermore, its asymptotic velocity satisfies the differential equation*

$$\dot{v}^{f,k} = \sum_{i=1}^N \pi_i \beta_{i,0}^k. \quad (4.1.3)$$

Proof

Balancing the terms of order ϵ^{-1} in (4.1.1), we obtain that

$$\alpha_{i,0}(t)(\bar{v}_{i,0}(t) - v_{i,0}(t)) = 0. \quad (4.1.4)$$

This means that $\alpha_{i,0} = 0$ or $\bar{v}_{i,0} - v_{i,0} = 0$. since $\underline{\alpha} = \min \alpha_i > 0$ see lemma 4, we have that $\bar{v}_{i,0} = v_{i,0}$. Therefore

$$\sum_{j=1}^N \phi_{ij}(x_0)v_{j,0} = v_{i,0}$$

and hence

$$\sum_{j=1}^N \phi_{ij}(x_0) v_{j,0}^k = v_{i,0}^k$$

Fixing a component $1 \leq k \leq d$ and writing the previous equation for all agents, we obtain

$$P(t) v_0^k(t) = v_0^k(t), \quad (4.1.5)$$

where the matrix P is given by:

$$P = \begin{bmatrix} \phi_{11}(x_0) & \cdots & \phi_{1N}(x_0) \\ \vdots & \ddots & \vdots \\ \phi_{N1}(x_0) & \cdots & \phi_{NN}(x_0) \end{bmatrix}, \quad (4.1.6)$$

and $v_0^k = (v_{1,0}^k, \dots, v_{N,0}^k) \quad \forall k = 1, \dots, d$. Since $P_{ij} = \phi_{ij} > 0$ and $\sum_{j=1}^N P_{ij} = 1$, the matrix P is a stochastic matrix. Since $P_{ij} > 0$ for all i, j , P has eigenvector $e = (1, \dots, 1)^t$ corresponding to the eigenvalue 1 of multiplicity one. Thus for each $k = 1, \dots, d$, equation (4.1.5) has a unique solution for v_0^k which is a multiple of $e = (1, \dots, 1)^t$. That is $v_0^k = c_k e$, where $c_k \in \mathbb{R}$. This shows that $v_{i,0}(t)$ are all equal for $i = 1, \dots, N$. This prove alignment in the velocity space. We shall denote this flocking velocity by $v^f(t)$.

Balancing the terms of order ϵ^0 in (4.1.1) gives the system

$$\dot{x}_{i,0}(t) = v_{i,0}(t), \quad (4.1.7)$$

$$\dot{v}_{i,0}(t) = \alpha_{i,1}(\bar{v}_{i,0}(t) - v_{i,0}(t)) + \alpha_{i,0}(\bar{v}_{i,1}(t) - v_{i,1}(t)) + \beta_{i,0}(t).$$

Since $v_{i,0} = v^f$ for all i , it follows that $\bar{v}_{i,0} = v^f$ for all i , and hence, from (4.1.2) we

obtain that

$$\bar{v}_{i,1} = \sum_{j=1}^N \phi_{ij}(x_0) v_{j,1} + \sum_{j=1}^N \left\{ \sum_{l=1}^N \sum_{k=1}^d \frac{\partial \phi_{ij}}{\partial x_l^k}(x_0) x_{l,1}^k \right\} v^f.$$

When we change the order of the summation in the second term and use the condition $\sum_{j=1}^N \phi_{i,j}(x) = 1$ to obtain that

$$\sum_{j=1}^N \left\{ \sum_{l=1}^N \sum_{k=1}^d \frac{\partial}{\partial x_l^k} \phi_{ij}(x_0) x_{l,1}^k \right\} v^f = \sum_{l=1}^N \left\{ \sum_{k=1}^d x_{l,1}^k \frac{\partial}{\partial x_l^k} \left(\sum_{j=1}^d \phi_{i,j}(x_0) \right) \right\} v^f = 0.$$

Thus

$$\bar{v}_{i,1} = \sum_{j=1}^N \phi_{ij}(x_0) v_{j,1}.$$

Substituting these results in equation (4.1.7), we have that for each i

$$\begin{aligned} \dot{v}^f &= \alpha_{i,0}(\bar{v}_{i,1} - v_{i,1}) + \beta_{i,0} \\ &= \alpha_{i,0} \left(\sum_{j=1}^N \phi_{ij}(x_0) v_{j,1} - v_{i,1} \right) + \beta_{i,0} \end{aligned} \tag{4.1.8}$$

From the first equation of (4.1.7) we have that

$$\dot{x}_{i,0} = v_{i,0} = v^f.$$

This implies that for each i

$$x_{i,0}(t) = x_{i,0}(0) + \int_0^t v^f(s) ds. \tag{4.1.9}$$

Hence for all i and j

$$x_{i,0}(t) - x_{j,0}(t) = x_{i,0}(0) - x_{j,0}(0). \tag{4.1.10}$$

It follows from (4.1.10) that the leading order relative positions of agents do not change with time. Hence by the shift invariant assumption on ϕ_{ij} , it follows that $\phi_{ij}(x_0(t))$ is independent of t .

We denote by \bar{a}_{ij} :

$$\bar{a}_{ij} = \phi_{ij}(x_0) \quad \forall i, j.$$

Since $\bar{v}_{i,0} = v_{i,0}$, it follows that $\alpha_{i,0} = \xi_i(\bar{v}_{i,0} - v_{i,0}) = \xi_i(0) > 0$. Hence, for each i ,

$$\dot{v}^f = \xi_i(0) \left(\sum_{j=1}^N \bar{a}_{ij} v_{j,1} - v_{i,1} \right) + \beta_{i,0}. \quad (4.1.11)$$

Taking the k th component in equation (4.1.11) we have that

$$\dot{v}^{f,k} = \xi_i(0) \left(\sum_{j=1}^N \bar{a}_{ij} v_{j,1}^k - v_{i,1}^k \right) + \beta_{i,0}^k, \quad (4.1.12)$$

for $k = 1, \dots, d$. We define for $1 \leq i, j \leq N$

$$q_{ij} = \xi_i(0) \bar{a}_{ij} \quad \forall i \neq j,$$

$$q_{ii} = \xi_i(0) \bar{a}_{ii} - \xi_i(0).$$

The matrix $Q = [q_{ij}]$ is a transition rate matrix of a continuous time Markov chain.

Moreover, since $q_{ij} = \xi_i(0) \bar{a}_{ij} > 0$ for all $i \neq j$, the matrix Q corresponds to an ergodic Markov chain in continuous time. Thus there exists a unique vector $(\pi_i)_{i=1}^N$ such that $\sum_{i=1}^N \pi_i = 1$ and

$$\sum_{i=1}^N \pi_i q_{ij} = 0.$$

With the introduction of matrix Q , (4.1.12) may be written as

$$\dot{v}^{f,k} = \sum_{j=1}^N q_{ij} v_{j,1}^k + \beta_{i,0}^k.$$

Multiplying by π_i and summing over $i = 1 \dots N$, and using properties of q_{ij} and π_i we obtain that

$$\dot{v}^{f,k} = \sum_{i=1}^N \pi_i \beta_{i,0}^k. \quad (4.1.13)$$

Hence the flocking velocity $v^f(t)$ evolves according to the equation

$$\dot{v}^f = \sum_{i=1}^N \pi_i \beta_{i,0}. \quad (4.1.14)$$

■

Remark 4 *We note from equation (4.1.14) that if $\beta = 0$, then the asymptotic velocity is a constant vector. Which is the case of many models that we have in the literature.*

In general, one may expect the steering terms β_i to depend on x_i, v_i and possible t , so that

$$\beta_i(t) = \eta_i(x_i(t), v_i(t), t) \quad (4.1.15)$$

where we suppose $\eta_i : \mathbb{R}^d \times \mathbb{R}^d \times [0, \infty) \rightarrow \mathbb{R}^d$ is C^1 in its arguments. Then, it follows that the evolution equation for v^f is given by

$$\dot{v}^f(t) = \sum_{j=1}^N \pi_j(x_0(t)) \eta_j(x_{0,j}(t), v^f(t), t), \quad (4.1.16)$$

where $x_{i,0}(t)$ are given by

$$x_0(t) = x(0) + \int_0^t v^f(s) ds. \quad (4.1.17)$$

Here $x(0) = (x_1(0), \dots, x_N(0))$ is the initial position of the agents and we observe that $\pi_i(x_0(t))$ is constant in time since $\phi_{ij}(x_0(t))$ is constant in time. We may summarize the leading order time evolution by the system of ODEs

$$\begin{aligned}\dot{x}_{i,0}(t) &= v^f(t), \\ \dot{v}^f(t) &= \sum_{j=1}^N \pi_i(x_0(t)) \eta_i(x_{0,i}(t), v^f(t), t).\end{aligned}\tag{4.1.18}$$

This is a $(N+1)d$ dimensional system and the leading order velocities are given by $v_{i,0}(t) = v^f(t)$. We observe that in order to obtain a unique solution, we need an initial condition for $v^f(0)$ which may not be the true initial velocities $v_i(0)$ of the agents. Intuitively, one expects a rapid initial transient layer during which flocking occurs and the agents reach the flocking velocity $v^f(0)$. In the next subsection, we scale time to investigate this transient layer.

4.2 Initial Transient Layer

The given problem has initial condition, $x(0) = (x_1(0), \dots, x_N(0))$ and $v(0) = (v_1(0), \dots, v_N(0))$. It is clear that $v^f(0)$ and $v_i(0)$ are not always equal. We then need to compute the initial velocity to solve (4.1.3)

We zoom into the transient layer at $t = 0$ by introducing the variable $\tau = t/\epsilon$.

We define X and V by

$$X(\tau, \epsilon) = x(t, \epsilon) = x(\epsilon\tau, \epsilon) \quad \text{and} \quad V(\tau, \epsilon) = v(t, \epsilon) = v(\epsilon\tau, \epsilon).$$

Differentiating with respect to τ , we have that

$$\frac{1}{\epsilon} \frac{dX_i(\tau, \epsilon)}{d\tau} = \frac{dx_i(t, \epsilon)}{dt}$$

and

$$\frac{1}{\epsilon} \frac{dV_i(\tau, \epsilon)}{d\tau} = \frac{dv_i(t, \epsilon)}{dt}$$

With the change of variable we have the following system of differential equations:

$$X'_i = \epsilon V_i, \tag{4.2.1}$$

$$V'_i = \alpha_i(\bar{V}_i - V_i) + \epsilon \beta_i,$$

where the prime denotes differentiation with respect to τ . The initial conditions to impose are

$$\begin{aligned} X_i(0) &= x_i(0), \\ V_i(0) &= v_i(0). \end{aligned} \tag{4.2.2}$$

As before, we assume an ϵ -expansion for X_i and V_i of the following form:

$$\begin{aligned} X_i(\tau, \epsilon) &= X_{i,0}(\tau, \epsilon) + \epsilon X_{i,1}(\tau, \epsilon) + \dots \\ V_i(\tau, \epsilon) &= V_{i,0}(\tau, \epsilon) + \epsilon V_{i,1}(\tau, \epsilon) + \dots \end{aligned} \tag{4.2.3}$$

Substituting this expansion in (4.2.1) we obtain

$$\begin{aligned} X'_{i,0} + \epsilon X'_{i,1} + \dots &= \epsilon(V_{i,0} + \epsilon V_{i,1} + \dots), \\ V'_{i,0} + \epsilon V'_{i,1} + \dots &= (\alpha_{i,0} + \epsilon \alpha_{i,1} + \dots)((\bar{V}_{i,0} - V_{i,0}) + \epsilon(\bar{V}_{i,1} - V_{i,1}) \dots), \\ &+ \epsilon(\beta_{i,0} + \epsilon \beta_{i,1} + \dots). \end{aligned}$$

Balancing the ϵ^0 terms, we find that

$$\begin{aligned} X'_{i,0} &= 0, \\ V'_{i,0} &= \alpha_{i,0}(\bar{V}_{i,0} - V_{i,0}). \end{aligned} \tag{4.2.4}$$

It follows that $X_{i,0}(\tau) = X_i(0) = x_i(0)$. This means that during the initial transient the leading order positions do not change in time τ .

The model (4.2.4) is similar to (2.6.2) without the steering terms, except that the positions $X_{i,0}$ are fixed. Hence the influence matrix $a_{ij} = \phi_{ij}(X_0)$ is constant and strictly positive. Defining

$$d_X(\tau) = \max_{i,j} \|X_{i,0}(\tau) - X_{j,0}(\tau)\|, \quad d_V(\tau) = \max_{i,j} \|V_{i,0}(\tau) - V_{j,0}(\tau)\|,$$

to be the diameters in the position and the velocity spaces respectively, we see that the assumptions of Lemma 4 and Theorem 2 are satisfied since the diameter in the steering space is zero. Thus Theorem 2 can be invoked to conclude that $d_V(\tau) \rightarrow 0$ as $\tau \rightarrow \infty$.

Now let us find $\lim_{\tau \rightarrow \infty} V_{i,0}(\tau)$. The second equation of (4.2.4) is

$$V'_{i,0} = \alpha_{i,0}(\bar{V}_{i,0} - V_{i,0}) = \alpha_{i,0} \left(\sum_{j=1}^N \phi_{ij}(X_0) V_{j,0} - V_{i,0} \right) = \sum_{j=1}^N q_{ij} V_{j,0}.$$

Where $Q = (q_{ij})$ is the same matrix that we have used in (4.1.12). Taking the k th components and letting $Z_i^k = V_{i,0}^k$ and $Z^k = (Z_1^k, \dots, Z_N^k)$ we have $Z'^k = Q Z^k$.

That is

$$Z_i'^k = \sum_{j=1}^N q_{ij} Z_j^k.$$

Multiplying by π_i and sum it from 1 to N , we have

$$\sum_{i=1}^N \pi_i Z_i'^k = \sum_{i=1}^N \sum_{j=1}^N \pi_i q_{ij} Z_j^k = \sum_{j=1}^N \left(\sum_{i=1}^N \pi_i q_{ij} \right) Z_j^k = 0.$$

This implies that for $\tau \geq 0$,

$$\sum_{i=1}^N \pi_i Z_i^k(\tau) = \sum_{i=1}^N \pi_i Z_i^k(0). \quad (4.2.5)$$

However, all the eigenvalues of Q except for one zero eigenvalue have negative real parts. Thus $Z^k(\tau) \rightarrow \bar{Z}^k$ where \bar{Z}^k is a multiple of $(1, \dots, 1)^t$. That is $\bar{Z}_k = c_k(1, \dots, 1)^t$. To find c_k , we take limits in (4.2.5):

$$\lim_{\tau \rightarrow \infty} \sum_{i=1}^N \pi_i Z_i^k(\tau) = c_k = \sum_{i=1}^N \pi_i Z_i^k(0) = \sum_{i=1}^N \pi_i V_{i,0}^k(0).$$

Using the standard matching condition, we deduce that

$$v^f(0) = \lim_{\tau \rightarrow \infty} V_{i,0}(\tau) = (c_1, \dots, c_d) = \left(\sum_{i=1}^N \pi_i V_{i,0}^1(0), \dots, \sum_{i=1}^N \pi_i V_{i,0}^d(0) \right). \quad (4.2.6)$$

Equation (4.2.6) helps to solve the differential equation (4.1.14). We have

$$v^f(t) = v^f(0) + \int_0^t \sum_{i=1}^N \pi_i \beta_{i,0}^k. \quad (4.2.7)$$

4.3 Numerical examples

In this section, we present some numerical simulations to illustrate our theoretical analysis. Moreover, we will compare the simulation of the solution of the perturb model with the original model for different values of ϵ . We consider a collection of $N = 7$ agents in two dimensions. We shall choose the initial positions and initial velocities randomly inside square regions $[0, 8] \times [0, 8]$ in position and $[0, 3] \times [0, 3]$ in velocity spaces respectively.

We assume all agents wish to follow the same trajectory

$$y(t) = (100 + 10 \sin(0.1t), 10 + 10 \cos(0.1t))^t$$

in the position space. We assume each agent i implements a PD (Proportional-Derivative) control feedback law for steering according to

$$\beta_i(t) = \gamma_1(\dot{y}(t) - v_i(t)) + \gamma_2(y(t) - x_i(t)),$$

where γ_1 and γ_2 are two parameters.

4.3.1 Choice of the Parameters γ_1 and γ_2

In this subsection, we want to determine the optimal value of the parameters that will control the overshoot. To this end, we will analyze the case of one agent. Vectors x and v represent its position and its velocity at time t . We want to control this agent such that it will steer towards the trajectory $y(t)$. To this end, we define the following control model.

$$\begin{aligned}\dot{x} &= v \\ \dot{v} &= \gamma_1(\dot{y} - v) + \gamma_2(y - x).\end{aligned}\tag{4.3.1}$$

Combining these two equations, we have the following second order differential equation:

$$\ddot{x} + \gamma_1\dot{x} + \gamma_2x = \gamma_1\dot{y} + \gamma_2y.\tag{4.3.2}$$

Let us recall some Laplace Transform formulae that will help our analysis:

$$\mathcal{L}(\ddot{x})(s) = s^2X - sx(0) - \dot{x}(0); \quad \mathcal{L}(\dot{x})(s) = sX - x(0)$$

$$\mathcal{L}(\dot{y})(s) = sY - y(0); \quad \mathcal{L}(x)(s) = X.$$

Applying the Laplace operator on equation(4.3.2), we have that

$$s^2X - sx(0) - \dot{x}(0) + \gamma_1(sX - x(0)) + \gamma_2X(s) = \gamma_1(sY - y(0)) + \gamma_2Y.$$

After some algebraic manipulation, we obtain the following

$$X = \frac{\gamma_1}{s^2 + \gamma_1s + \gamma_2}sY + \frac{\gamma_2}{s^2 + \gamma_1s + \gamma_2}Y + \frac{\dot{x}(0) + \gamma_1x(0) + sx(0) - \gamma_1y(0)}{s^2 + \gamma_1s + \gamma_2}.$$

We define $o(t) = v(t) - \dot{y}(t)$ the quantity that will control the overshoot of the velocity $v(t)$ w.r.t the target velocity $\dot{y}(t)$. Taking the Laplace transform of the function $o(t)$, we have;

$$\begin{aligned} O(s) &= sX - x(0) - sY + y(0) \\ &= s(X - Y) - x(0) + y(0) \\ &= \frac{\gamma_1}{s^2 + \gamma_1s + \gamma_2}s^2Y + \frac{\gamma_2}{s^2 + \gamma_1s + \gamma_2}sY + \frac{\dot{x}(0) + \gamma_1x(0) + sx(0) - \gamma_1y(0)}{s^2 + \gamma_1s + \gamma_2}s \\ &\quad - x(0) - sY - y(0) \\ &= \frac{\gamma_1}{s^2 + \gamma_1s + \gamma_2}s^2Y + \left(\frac{\gamma_2}{s^2 + \gamma_1s + \gamma_2} - 1\right)sY \\ &\quad + \frac{\dot{x}(0) + \gamma_1x(0) + sx(0) - \gamma_1y(0)}{s^2 + \gamma_1s + \gamma_2}s - x(0) + y(0) \end{aligned}$$

$$\begin{aligned}
&= -\frac{s}{s^2 + \gamma_1 s + \gamma_2} s^2 Y + \frac{\dot{x}(0) + \gamma_1 x(0) + s x(0) - \gamma_1 y(0)}{s^2 + \gamma_1 s + \gamma_2} s - x(0) + y(0) \\
&= -\frac{s}{s^2 + \gamma_1 s + \gamma_2} s^2 Y + \frac{s^2 y(0) + s \dot{x}(0) - \gamma_2 (x(0) - y(0))}{s^2 + \gamma_1 s + \gamma_2} \\
&= -\frac{s}{s^2 + \gamma_1 s + \gamma_2} s^2 Y + y(0) + (-\gamma_1 y(0) + x(0)) \frac{s}{s^2 + \gamma_1 s + \gamma_2} \\
&\quad + (-\gamma_2 - \gamma_1 (x(0) + y(0))) \frac{1}{s^2 + \gamma_1 s + \gamma_2}
\end{aligned}$$

Now, using the partial fractional technique, we have

$$\frac{1}{s^2 + \gamma_1 s + \gamma_2} = \frac{1}{\lambda_1 - \lambda_2} \frac{1}{s - \lambda_1} - \frac{1}{\lambda_1 - \lambda_2} \frac{1}{s - \lambda_2}.$$

and

$$\frac{s}{s^2 + \gamma_1 s + \gamma_2} = \frac{\lambda_1}{\lambda_1 - \lambda_2} \frac{1}{s - \lambda_1} - \frac{\lambda_2}{\lambda_1 - \lambda_2} \frac{1}{s - \lambda_2}.$$

Here λ_1 and λ_2 are roots of the quadratic equation $s^2 + \gamma_1 s + \gamma_2 = 0$.

$O(s)$ can be written as

$$O(s) = -\frac{s}{s^2 + \gamma_1 s + \gamma_2} s^2 Y + K_1 \frac{s}{s^2 + \gamma_1 s + \gamma_2} + K_2 \frac{1}{s^2 + \gamma_1 s + \gamma_2} + y(0),$$

where $K_1 = -\gamma_1 y(0) + x(0)$ and $K_2 = -\gamma_2 - \gamma_1 (x(0) + y(0))$ are two constant vectors

depending on initial conditions.

$$\begin{aligned}
O(s) &= \left(\frac{\lambda_1}{\lambda_1 - \lambda_2} \frac{1}{s - \lambda_1} - \frac{\lambda_2}{\lambda_1 - \lambda_2} \frac{1}{s - \lambda_2} \right) s^2 Y \\
&\quad + K_1 \left(\frac{\lambda_1}{\lambda_1 - \lambda_2} \frac{1}{s - \lambda_1} - \frac{\lambda_2}{\lambda_1 - \lambda_2} \frac{1}{s - \lambda_2} \right) + K_2 \left(\frac{1}{\lambda_1 - \lambda_2} \frac{1}{s - \lambda_1} - \frac{1}{\lambda_1 - \lambda_2} \frac{1}{s - \lambda_2} \right) + y(0).
\end{aligned}$$

Taking the inverse Laplace transform of O ,

$$\begin{aligned}
o(t) &= \frac{\lambda_1}{\lambda_1 - \lambda_2} e^{\lambda_1 t} * \ddot{y}(t) - \frac{\lambda_2}{\lambda_1 - \lambda_2} e^{\lambda_2 t} * \ddot{y}(t) \\
&\quad + K_1 \frac{\lambda_1}{\lambda_1 - \lambda_2} e^{\lambda_1 t} - K_1 \frac{\lambda_2}{\lambda_1 - \lambda_2} e^{\lambda_2 t} + K_2 \frac{1}{\lambda_1 - \lambda_2} e^{\lambda_1 t} - K_2 \frac{1}{\lambda_1 - \lambda_2} e^{\lambda_2 t} + y(0).
\end{aligned}$$

Grouping like terms, we have

$$\begin{aligned}
o(t) &= \frac{\lambda_1}{\lambda_1 - \lambda_2} e^{\lambda_1 t} * \ddot{y}(t) - \frac{\lambda_2}{\lambda_1 - \lambda_2} e^{\lambda_2 t} * \ddot{y}(t) \\
&\quad + (K_1 \frac{\lambda_1}{\lambda_1 - \lambda_2} + K_2 \frac{1}{\lambda_1 - \lambda_2}) e^{\lambda_1 t} - (K_1 \frac{\lambda_2}{\lambda_1 - \lambda_2} + K_2 \frac{1}{\lambda_1 - \lambda_2}) e^{\lambda_2 t} + y(0).
\end{aligned} \tag{4.3.3}$$

The objective here is to see how we can choose γ_1 and γ_2 so that we can control the overshoot. Hence,

$$e^{\lambda_i t} * \ddot{y}(t) = \int_0^t e^{\lambda_i s} \ddot{y}(t-s) ds \quad \text{and} \quad e^{\lambda_i t} * \dot{y}(t) = \int_0^t e^{\lambda_i s} \dot{y}(t-s) ds. \tag{4.3.4}$$

We further assume that there exist M_1 and M_2 such that:

$$\|\dot{y}(t)\| \leq M_1 \quad \text{and} \quad \|\ddot{y}(t)\| \leq M_2$$

We then have:

$$\|e^{\lambda_i t} * \ddot{y}(t)\| \leq M_i \int_0^t e^{\lambda_i s} ds \leq \frac{M_i}{|\lambda_i|} (1 - e^{\lambda_i t}) \leq \frac{M_i}{|\lambda_i|} \quad \text{since} \quad \lambda_i < 0.$$

Also, we have $e^{\lambda_i t} \leq 1 \quad \forall i = 1, 2$. With these upper bounds, we have after using the triangle inequality, an upper bound of $o(t)$ is giving by:

$$\begin{aligned}
|o(t)| &\leq \frac{|\lambda_1|}{|\lambda_1 - \lambda_2|} \frac{M_1}{|\lambda_1|} + \frac{|\lambda_2|}{|\lambda_1 - \lambda_2|} \frac{M_2}{|\lambda_2|} \\
&\quad + \left(\frac{\|K_1\| |\lambda_1|}{|\lambda_1 - \lambda_2|} + \frac{\|K_2\|}{|\lambda_1 - \lambda_2|} \right) + \left(\frac{\|K_1\| |\lambda_2|}{|\lambda_1 - \lambda_2|} + \frac{\|K_2\|}{|\lambda_1 - \lambda_2|} \right) + \|y(0)\|.
\end{aligned} \tag{4.3.5}$$

The factors $\frac{1}{|\lambda_i|}$ or $\frac{1}{\lambda_1 - \lambda_2}$ appear on all terms and they may be a determinant factor on the analysis of the overshoot.

$$\lambda_1 = \frac{-\gamma_1 + \sqrt{\gamma_1^2 - 4\gamma_2}}{2} \quad \text{and} \quad \lambda_2 = \frac{-\gamma_1 - \sqrt{\gamma_1^2 - 4\gamma_2}}{2}$$

are solution of the equation $s^2 + \gamma_1 s + \gamma_2 = 0$ and

$$\lambda_1 - \lambda_2 = \sqrt{\gamma_1^2 - 4\gamma_2}.$$

Let us define r as $\gamma_1^2 = 4r\gamma_2$. Now ,

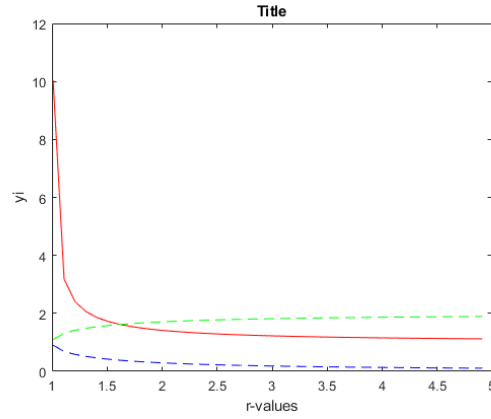
$$\frac{1}{\lambda_1 - \lambda_2} = \frac{1}{\gamma_1 \sqrt{1 - \frac{1}{r}}}$$

$$|\lambda_1| = \left| -\gamma_1 + \sqrt{\gamma_1^2 - 4\gamma_2} \right| = \gamma_1 \left| -1 + \sqrt{1 - \frac{1}{r}} \right|$$

$$|\lambda_2| = \left| -\gamma_1 - \sqrt{\gamma_1^2 - 4\gamma_2} \right| = \gamma_1 \left| 1 + \sqrt{1 - \frac{1}{r}} \right|$$

We will plot these functions of r to see with values of r will help us to reduce the overshoot that may appear on $v(t)$.

Figure 4.1: y_1 in red, y_2 in green and y_3 in blue



$$y_1 = \frac{1}{\lambda_1 - \lambda_2}; \quad y_2 = \frac{1}{|\lambda_2|}; \quad y_3 = \frac{1}{|\lambda_1|}.$$

From the figure 4.1, we read that, when $r \geq 1.7$ the functions y_1, y_2 and y_3 are small.

4.3.2 Simulations

In these MATLAB simulations, we take $\gamma_1 = 2$ and $\gamma_2 = 0.1$. We computed the solutions of the full model (2.6.2) for $\epsilon = 0.1$, $\epsilon = 0.01$ and $\epsilon = 0.001$. Additionally, we also computed the solution of the reduced model (4.1.18) obtained via the singular perturbation theory. In order to compute the correct initial flocking velocity $v^f(0)$ to be used in conjunction with (4.1.18), we use the equation (4.2.6). Finally, we computed the leading order approximation and compared it to the simulation when $\epsilon = 0.1$, $\epsilon = 0.01$ and $\epsilon = 0.001$. For all ϵ , we used the same randomly chosen initial conditions which we provide here. Initial positions were

$$\begin{aligned} x_1(0) &= (6.8897, 7.1568)^t, & x_2(0) &= (1.6819, 4.4079)^t, & x_3(0) &= (4.0103, 5.8168)^t, \\ x_4(0) &= (6.3834, 6.7922)^t, & x_5(0) &= (2.4842, 6.1173)^t, & x_6(0) &= (5.8959, 1.4635)^t, \\ x_7(0) &= (1.0710, 4.4853)^t, \end{aligned}$$

and the initial velocities were

$$\begin{aligned} v_1(0) &= (2.8792, 1.0212)^t, & v_2(0) &= (1.7558, 0.6714)^t, & v_3(0) &= (2.2538, 0.7653)^t, \\ v_4(0) &= (1.5179, 2.0972)^t, & v_5(0) &= (2.6727, 2.8779)^t, & v_6(0) &= (1.6416, 0.4159)^t, \\ v_7(0) &= (0.4479, 0.7725)^t. \end{aligned}$$

In these simulations, we have used the following functions.

$$\begin{aligned} \phi_{ij}(x, u) &= \frac{\phi(r_{ij})}{\sum_k \phi(r_{ik})} \text{ where, } r_{ij} = \|x_j - x_i\| \\ \phi(r) &= \frac{1}{(1 + r^2)^{0.3}} \\ \alpha_i(t) = \xi_i(u_i) &= \frac{10}{(0.1 + \|u_i\|^2)^{0.5}} \text{ where, } u_i = \bar{v}_i - v_i. \end{aligned}$$

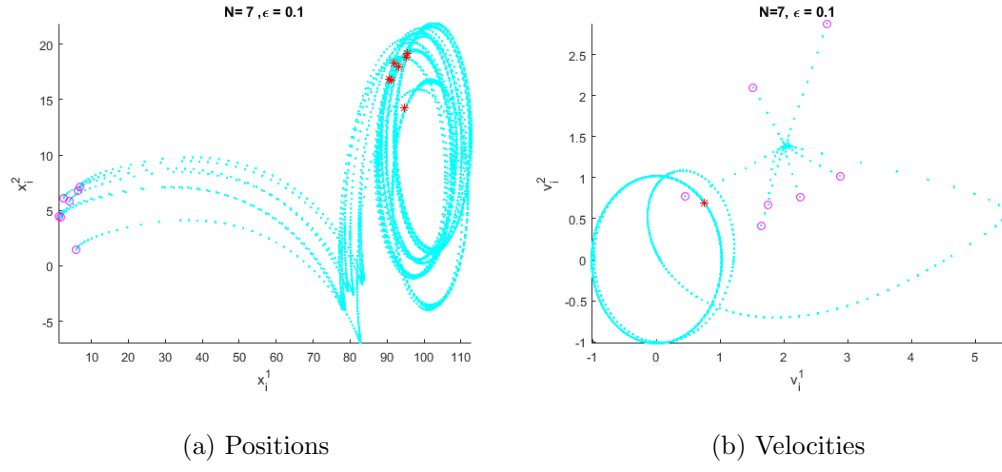
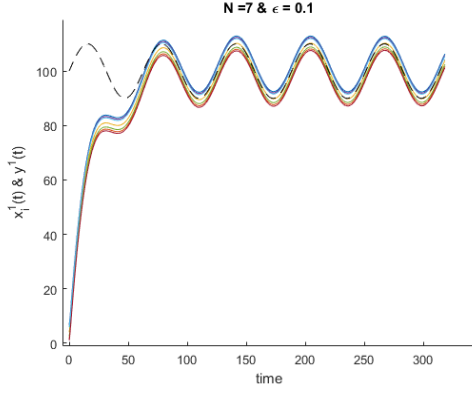
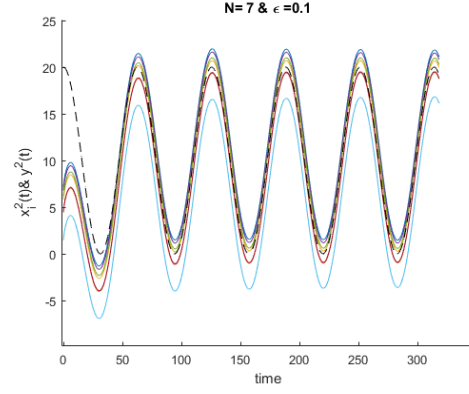


Figure 4.2: Trajectories in position and velocity spaces. Cyan circles represent initial values and red stars the final values. Case $\epsilon = 0.1$.

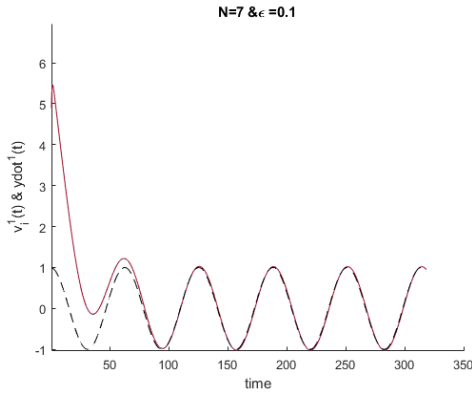


(a) $x_i^1(t)$ and $y^1(t)$

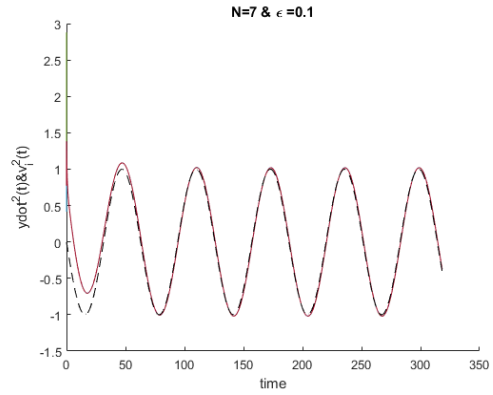


(b) $x_i^2(t)$ and $y^2(t)$

Figure 4.3: Positions against time. Case $\epsilon = 0.1$. Target trajectory in dash black.



(a) $v_i^1(t)$ and $\dot{y}^1(t)$



(b) $v_i^2(t)$ and $\dot{y}^2(t)$

Figure 4.4: Velocities against time. Case $\epsilon = 0.1$. Target velocity in dash black

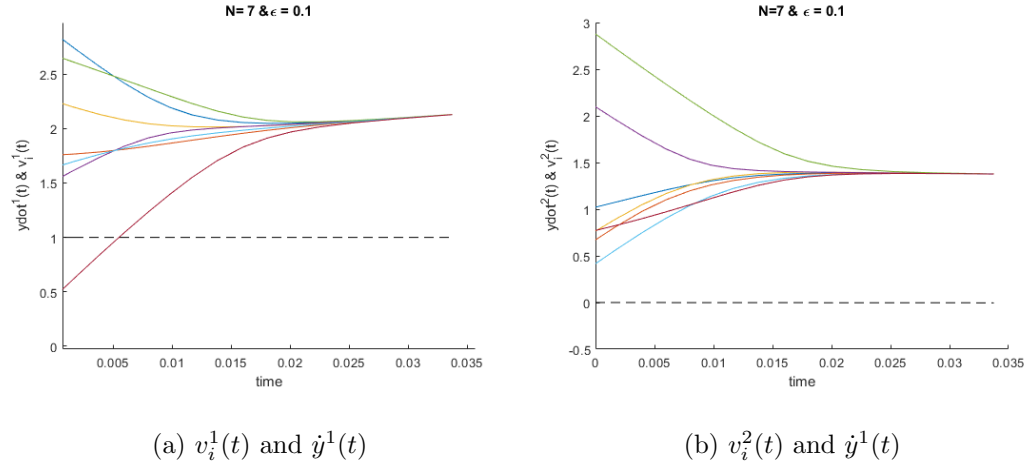


Figure 4.5: Velocities against time for t close to zero. Case $\epsilon = 0.1$ short representation.

Target velocity in dash black

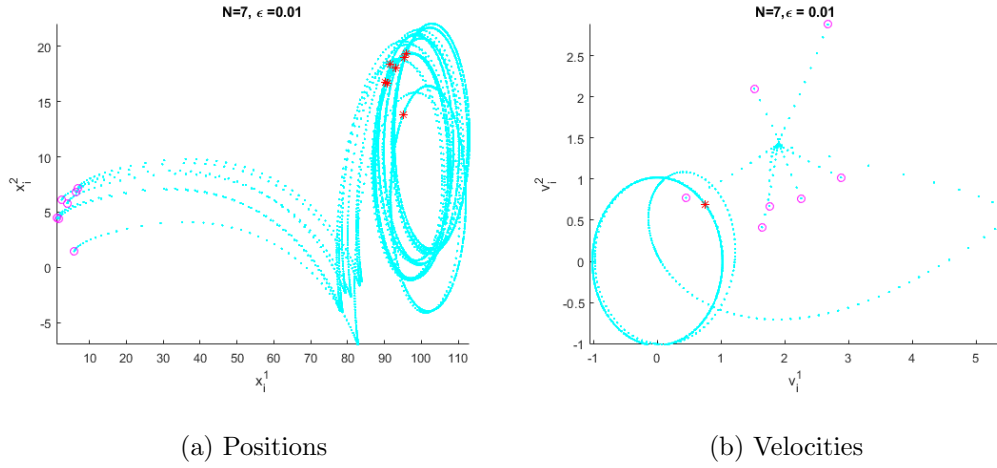
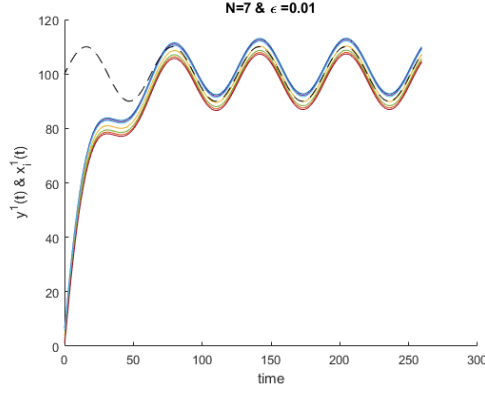
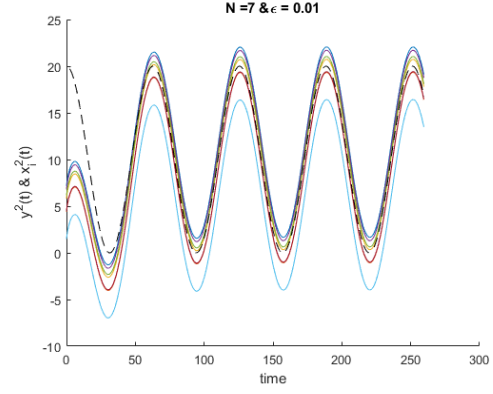


Figure 4.6: Trajectories in position and velocity spaces. Cyan circles represent initial values and red stars the final values.. Case $\epsilon = 0.01$.

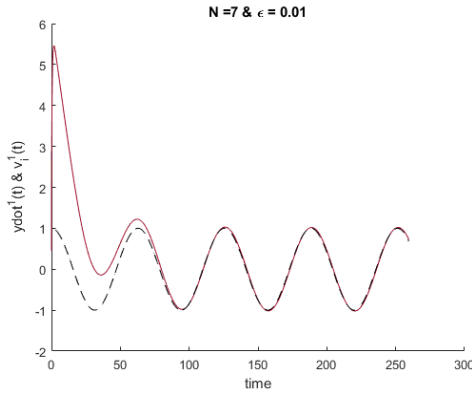


(a) $x_i^1(t)$ and $y^1(t)$

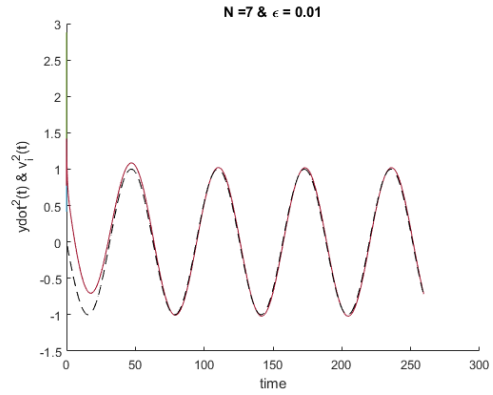


(b) $x_i^2(t)$ and $y^2(t)$

Figure 4.7: Trajectories against time. Case $\epsilon = 0.01$. Target trajectory in dash black



(a) $v_i^1(t)$ and $\dot{y}^1(t)$



(b) $v_i^2(t)$ and $\dot{y}^2(t)$

Figure 4.8: Velocities against time. Case $\epsilon = 0.01$. Target velocity in dash black

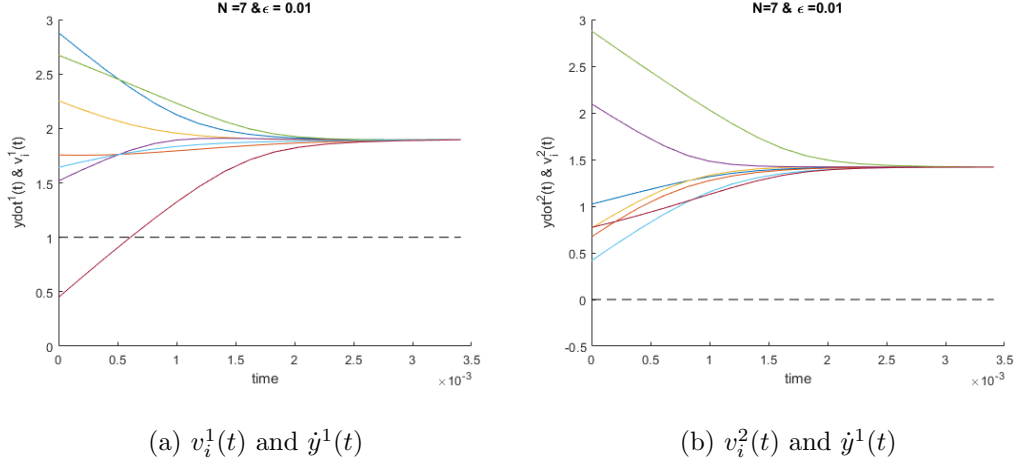


Figure 4.9: Velocities against time for t close to zero. Case $\epsilon = 0.01$. Target velocity in dash black

In the position and velocity spaces, the small cyan circles represent the initial values of our simulations and the stars represent the final time values. Figures 4.2, 4.6 and 4.10 show that our model flocks. In fact, Figures 4.2b, 4.6b and 4.10b show that all agents flock to a common velocity $V^f(0)$ and then stay together and steer towards the target velocity. Our simulations also show that after some time the trajectory of each agent is similar to the target trajectory which is a circle. Furthermore, Figures, 4.3, 4.7 and 4.11 which show the plots of trajectories components against time we see that after some time, all the components follow the target trajectory components (in dashed black). Figures 4.4, 4.8 and 4.12 is the plots of components velocities against time. In conjunction with figures 4.5, 4.9 and 4.13 we read that velocities components converge very fast to a common velocity and then in the long run, align with the target velocity (in dashed black).

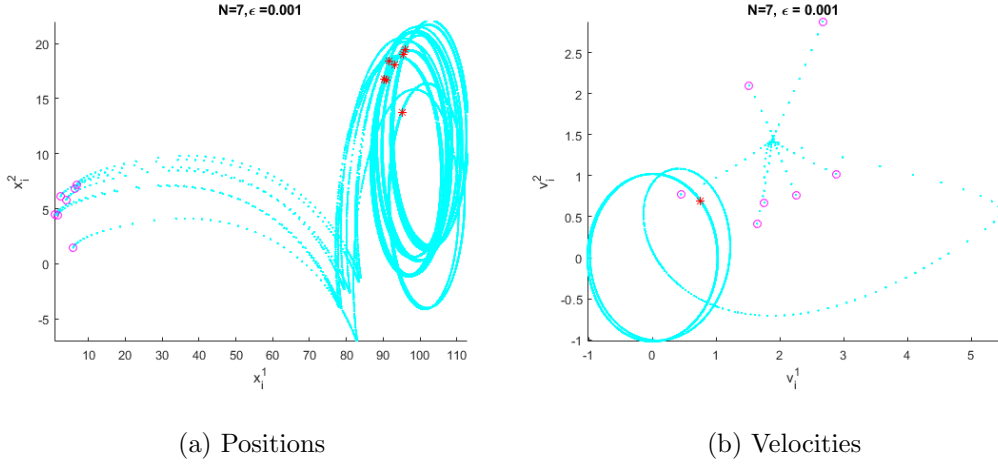


Figure 4.10: Trajectories in position and velocity spaces. Cyan circles represent initial values and red stars the final values.. Case $\epsilon = 0.001$.

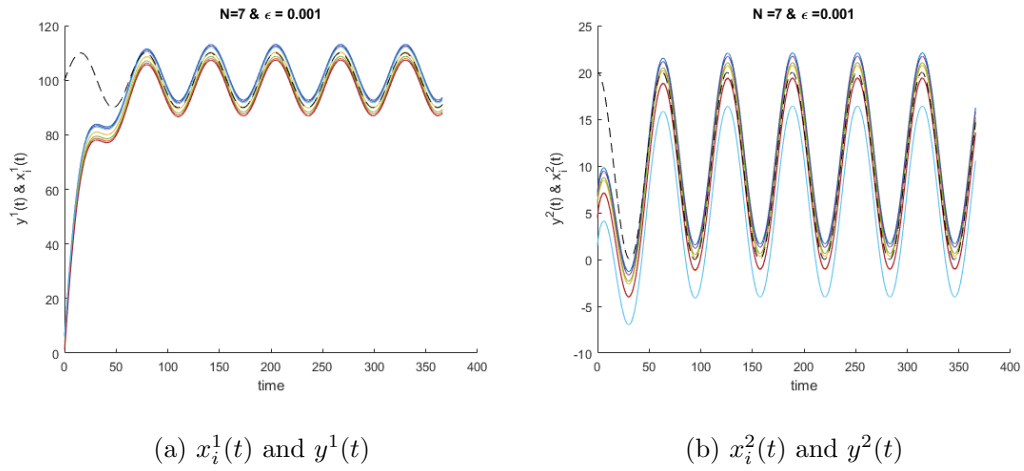
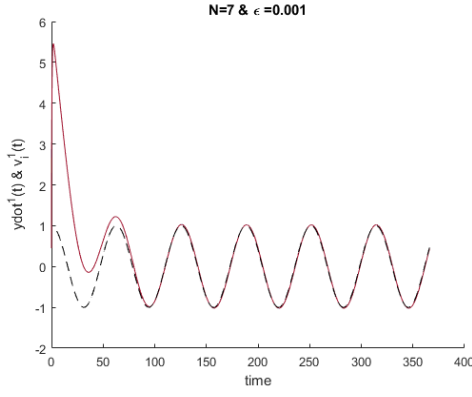
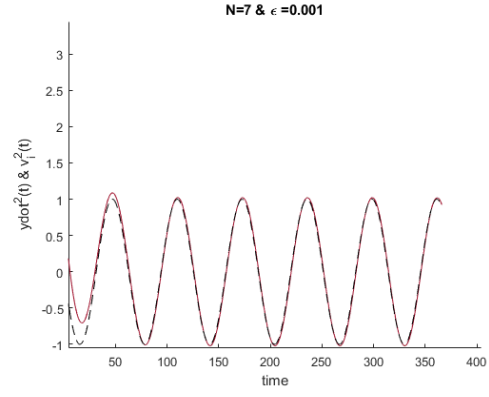


Figure 4.11: Positions against time. Case $\epsilon = 0.001$. Target trajectory in dash black

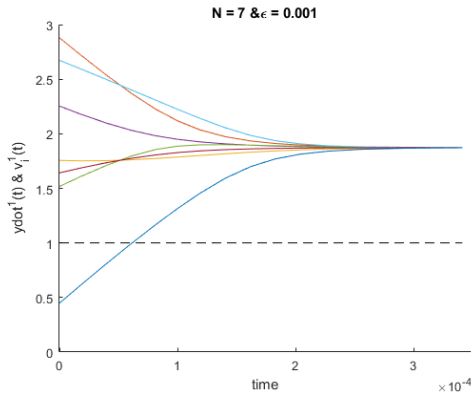


(a) $v_i^1(t)$ and $\dot{y}^1(t)$

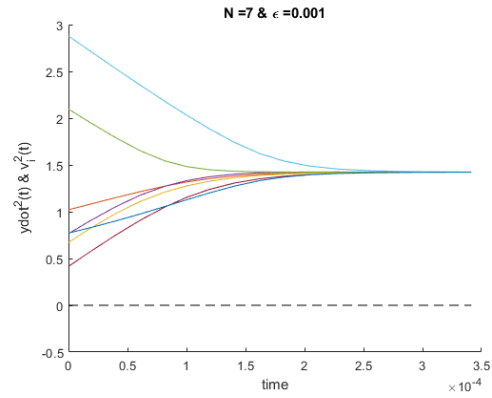


(b) $v_i^2(t)$ and $\dot{y}^2(t)$

Figure 4.12: Velocities against time. Case $\epsilon = 0.001$. Target velocity in dash black



(a) $v_i^1(t)$ and $\dot{y}^1(t)$



(b) $v_i^2(t)$ and $\dot{y}^1(t)$

Figure 4.13: Velocities against time for t close to zero. Case $\epsilon = 0.001$. Target velocity in dash black

Comparison of the leading order and the cases $\epsilon = 0.1$, $\epsilon = 0.01$ and $\epsilon = 0.001$ We graphically compare the positions and the velocities of the leading order approximation model (4.1.18) and the actual model (4.0.1) for different values of ϵ . In Figures 4.14 ,4.15 and 4.16, the approximate model solution is in green color while the actual model solution is in blue. The small red circles and red stars represent the initial and final positions for the actual model. Likewise, the small yellow circles and yellow stars represent the initial and final position for the approximate model. Graphically, we see that in the velocity space, all the initial velocity converges to one point and evolve similarly to the leading order approximation. Whereas, in the position space both have a similar trajectories.

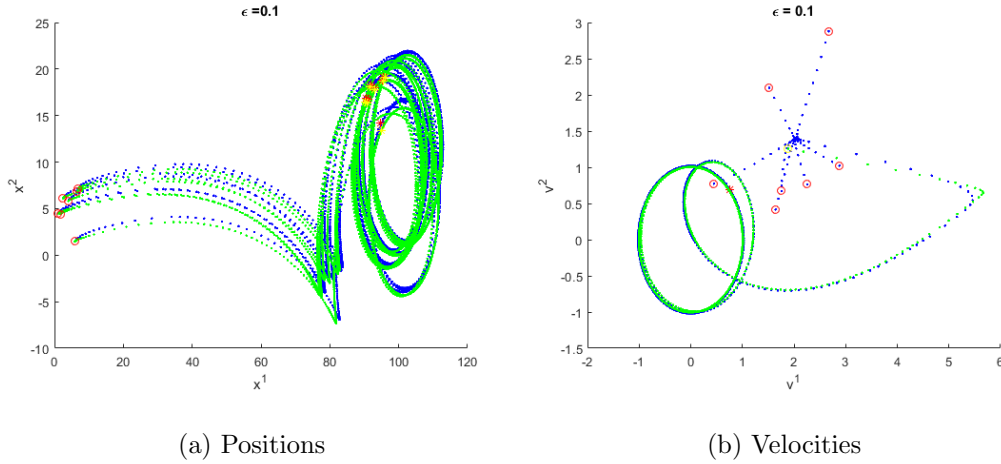


Figure 4.14: Comparison between the reduced model (in green) and exact solution (in blue) for $\epsilon = 0.1$

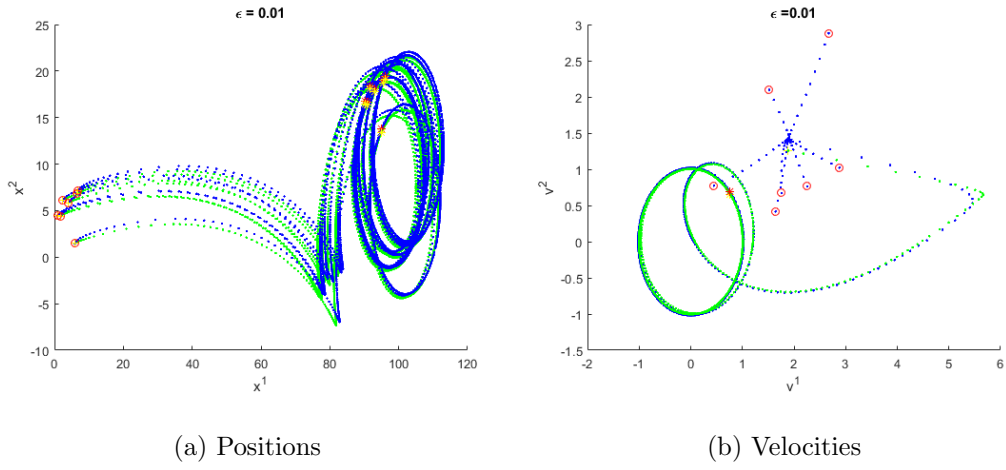


Figure 4.15: Comparison between the reduced model (green) and exact solution (in blue) for $\epsilon = 0.01$

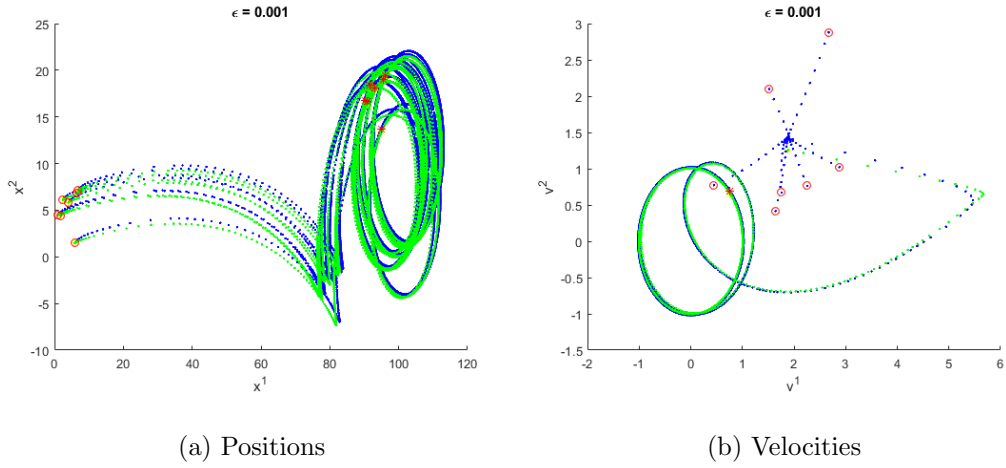


Figure 4.16: Comparison between the reduced model (in green) and exact solution (in blue) for $\epsilon = 0.001$

4.4 Analysis of the Singularly Perturbed Model

We formally studied the fast flocking and slow steering model via singular perturbation methods. Our simulations suggest that this model flocks very fast and steer towards a target trajectory. We have also compared the plots of the leading order solution and the exact solution for slow and fast model for different values of ϵ see Figures 4.14, 4.15 and, 4.16. Now, in this section, we want to study analytically the behavior of the model in the finite interval of time $[0, T]$ when the parameter ϵ approaches zero. We have the family of models given by:

$$\begin{aligned} \dot{x}_i &= v_i \\ \dot{v}_i &= \frac{\alpha_i}{\epsilon}(\bar{v}_i - v_i) + \beta_i \\ \bar{v}_i &= \sum_{j=1}^N \phi_{ij}(x) v_j \\ \alpha_i &= \xi_i(\bar{v}_i - v_i) \quad \forall i = 1, \dots, N. \end{aligned} \tag{4.4.1}$$

Where $\epsilon \in (0, 1]$. $x_i(t, \epsilon), v_i(t, \epsilon)$ are solutions of the model. $d_X(t, \epsilon)$ and $d_V(t, \epsilon)$ are the diameters in the trajectory and velocity space respectively. We will consider the closed loop model.

Assumption 4 $d_\beta(t, \epsilon)$ is uniformly bounded on every bounded interval $[0, T]$. That is, for each T there exist $M > 0$ such that $d_\beta(t, \epsilon) \leq M \quad \forall t \in [0, T]$ and $\epsilon \in (0, 1]$.

We recall the function ψ defined as:

$$\psi(r) = \min_{1 \leq i, j \leq N} \min\{\phi_{ij}(x; u) \mid \|x_l - x_k\| \leq r, u \in \bar{B}^d \text{ and } 1 \leq l, k \leq N\} \tag{4.4.2}$$

Theorem 3 Under assumption 4, for fixed $t_0 > 0$,

$$\lim_{\epsilon \rightarrow 0} d_V(t_0) \rightarrow 0 \quad \text{and} \quad \limsup_{\epsilon \rightarrow 0} d_X(t_0) \leq d_X(0).$$

Proof Pick $T > t_0$. From equation (3.3.3) we have for $t \in [0, T]$

$$\begin{aligned} \frac{d}{dt} d_X(t, \epsilon) &\leq d_V(t, \epsilon) \\ \frac{d}{dt} d_V(t, \epsilon) &\leq -\frac{\underline{\alpha}}{\epsilon} N^2 \psi(d_X(t, \epsilon)) d_V(t, \epsilon) + d_\beta(t, \epsilon). \end{aligned}$$

Here, $\underline{\alpha} = \inf_{i,t} \alpha_i(t) > 0$ where $t \in [0, T]$. Let us define the energy functional

$$\mathcal{E} : \mathbb{R} \times \mathbb{R} \times \mathbb{R} \rightarrow \mathbb{R}$$

$$\mathcal{E}(d_X(t, \epsilon), d_V(t, \epsilon), \epsilon) = d_V(t, \epsilon) + \frac{\underline{\alpha}}{\epsilon} N^2 \int_0^{d_X(t, \epsilon)} \psi(s) ds, \quad (4.4.3)$$

Its time derivative is :

$$\begin{aligned} \dot{\mathcal{E}} &= \dot{d}_V(t, \epsilon) + \frac{\underline{\alpha}}{\epsilon} N^2 \psi(d_X(t, \epsilon)) d_V(t, \epsilon) \\ &\leq -\frac{\underline{\alpha}}{\epsilon} N^2 \psi(d_X(t, \epsilon)) d_V(t, \epsilon) + d_\beta(t, \epsilon) + \frac{\underline{\alpha}}{\epsilon} N^2 \psi(d_X(t, \epsilon)) d_V(t, \epsilon) \\ &\leq d_\beta(t, \epsilon). \end{aligned}$$

Which implies that

$$\mathcal{E}(d_X(t, \epsilon), d_V(t, \epsilon), \epsilon) - \mathcal{E}(d_X(0), d_V(0), \epsilon) \leq \int_0^t d_\beta(s, \epsilon) ds.$$

That is,

$$d_V(t, \epsilon) \leq \frac{\underline{\alpha}}{\epsilon} N^2 \int_{d_X(t, \epsilon)}^{d_X(0)} \psi(s) ds + \int_0^t d_\beta(s, \epsilon) ds + d_V(0).$$

Let $d^* > d_X(0)$. Then there exist $\epsilon_0 > 0$ such that $\epsilon_0 \leq 1$, and for all $\epsilon \in (0, \epsilon_0]$

$$\int_0^t d_\beta(s, \epsilon) ds + d_V(0) \leq MT + d_V(0) \leq \frac{\underline{\alpha}}{\epsilon} N^2 \int_{d_X(0)}^{d^*} \psi(s) ds$$

$$\begin{aligned}
d_V(t, \epsilon) &\leq \frac{\alpha}{\epsilon} N^2 \int_{d_X(t, \epsilon)}^{d_X(0)} \psi(s) ds + \frac{\alpha}{\epsilon} N^2 \int_{d_X(0)}^{d^*} \psi(s) ds \\
d_V(t, \epsilon) &\leq \frac{\alpha}{\epsilon} N^2 \int_{d_X(t, \epsilon)}^{d^*} \psi(s) ds.
\end{aligned}$$

This implies that $d_X(t, \epsilon) \leq d^*$ for all t in $[0, T]$ and $\epsilon \in (0, \epsilon_0]$. Since ψ is decreasing we have ,

$$\psi(d_X(t, \epsilon)) \geq \psi(d^*) = \psi_*.$$

We then have

$$\frac{d}{dt} d_V(t, \epsilon) \leq -\frac{\alpha}{\epsilon} N^2 \psi_* d_V(t, \epsilon) + d_\beta(t, \epsilon).$$

Using Grönwall's inequality, we have

$$d_V(t, \epsilon) \leq e^{-\frac{\alpha}{\epsilon} N^2 \psi_* t} d_V(0) + \int_0^t e^{-\frac{\alpha}{\epsilon} N^2 \psi_* (t-s)} d_\beta(s, \epsilon) ds.$$

Then,

$$0 \leq \lim_{\epsilon \rightarrow 0} d_V(t, \epsilon) \leq \lim_{\epsilon \rightarrow 0} \left(e^{-\frac{\alpha}{\epsilon} N^2 \psi_* t} d_V(0) + \int_0^t e^{-\frac{\alpha}{\epsilon} N^2 \psi_* (t-s)} d_\beta(s, \epsilon) ds \right)$$

For $t \in (0, T]$ we have

$$\lim_{\epsilon \rightarrow 0} e^{-\frac{\alpha}{\epsilon} N^2 \psi_* t} = 0$$

and

$$\begin{aligned}
\lim_{\epsilon \rightarrow 0} \int_0^t e^{-\frac{\alpha}{\epsilon} N^2 \psi_* (t-s)} d_\beta(s, \epsilon) ds &= \int_0^t \lim_{\epsilon \rightarrow 0} e^{-\frac{\alpha}{\epsilon} N^2 \psi_* (t-s)} d_\beta(s, \epsilon) ds \\
&\leq M \int_0^t \lim_{\epsilon \rightarrow 0} e^{-\frac{\alpha}{\epsilon} N^2 \psi_* (t-s)} ds = 0.
\end{aligned}$$

Hence,

$$\lim_{\epsilon \rightarrow 0} d_V(t, \epsilon) = 0.$$

Note that at $t = 0$, $d_V(0, \epsilon) = d_V(0) \neq 0$. Now let analyze $d_X(t, \epsilon)$

$$\begin{aligned} d_X(t, \epsilon) - d_X(0) &\leq \int_0^t d_V(s, \epsilon) ds \\ &\leq \int_0^t e^{-\frac{\alpha}{\epsilon} N^2 \psi_* s} d_V(0) ds + \int_0^t \int_0^\tau e^{-\frac{\alpha}{\epsilon} N^2 \psi_*(\tau-s)} d_\beta(s, \epsilon) ds d\tau \end{aligned}$$

Taking the limit as $\epsilon \rightarrow 0$ and $t \in (0, T]$ we have:

$$\lim_{\epsilon \rightarrow 0} \int_0^t e^{-\frac{\alpha}{\epsilon} N^2 \psi_* s} d_V(0) ds = 0$$

and

$$\limsup_{\epsilon \rightarrow 0} \int_0^t \int_0^\tau e^{-\frac{\alpha}{\epsilon} N^2 \psi_*(\tau-s)} d_\beta(s, \epsilon) ds d\tau = 0.$$

And Hence

$$\limsup_{\epsilon \rightarrow 0} d_X(t, \epsilon) \leq d_X(0).$$

■

Chapter 5: A Generalized Model With Steering and Collision Avoidance Terms

The model we have studied so far has the alignment term and the steering term. None of these terms can prevent a collision. Indeed, in Chapter 3, we have studied our generalized model with steering. We showed that under certain conditions, the model flocks. In Chapter 4, we presented a fast flocking and slow steering model. Our simulations suggested that the model flocks. Moreover, we provided a flocking velocity of the leading order approximation. None of these suggested that our model can prevent collision. For instance, the plot of the minimum distance between agents shows that the minimum distance decreases as a function of time see figure 5.3 (blue graph). We think that for the purpose of the application, it will be necessary to further improve the quality of the model in a way that will prevent a collision from occurring. To this end, we will augment our model with an extra force. The objective of this chapter will be to simulate the ameliorated model and see the effect of the collision avoidance term that we have added. The new model

under study reads as:

$$\begin{aligned}\frac{dx_i}{dt} &= v_i \\ \frac{dv_i}{dt} &= \alpha_i(t)(\bar{v}_i - v_i) + \beta_i(t) + \text{extra force}\end{aligned}$$

5.1 Simulations of the Model with Extra Force Derived from Morse Potential

The Morse potential is used in physics to model the interaction between molecules. In a collection of N agents, the potential at agent i is giving by

$$V_i = \sum_{i \neq j} U(r_{ij}).$$

Where,

- $U(r_{ij}) = D(1 - \exp(-a(r_{ij} - r_0)))^2$ is the potential created by agent j on agent i .
- r_{ij} is the distance between agent i and agent j .
- $r_0 \neq 0$ is the desired distance between agent i and agent j at the equilibrium.

To fully describe the flocking phenomena, three properties are essential. Let us illustrate these properties by considering the case of two agents separated by the distance r_{ij} . We have

- Agents must avoid a collision; thus, repulsive force must occur when $r_{ij} < r_0$.

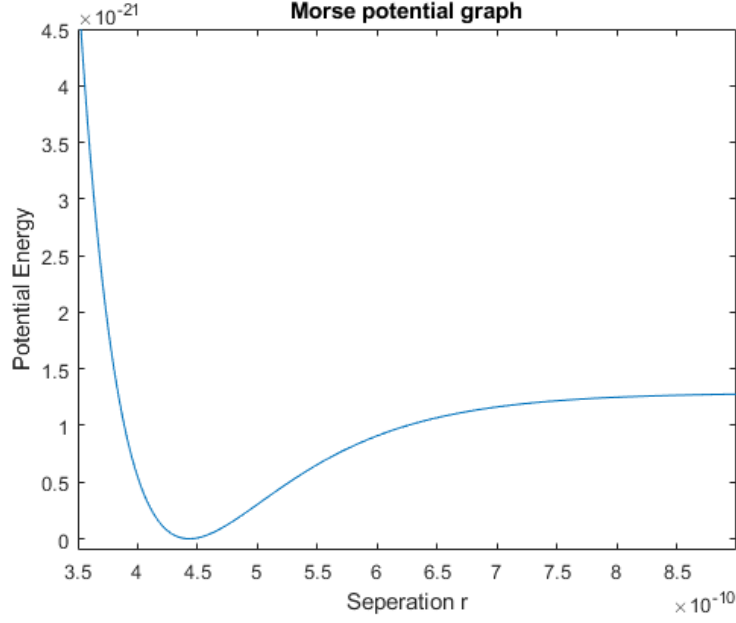


Figure 5.1: Morse potential graph

- Agents must stay apart from each other, that is $r_{ij} \geq r_0$.
- Agents must stay together, that is and attractive force must be maintained for $r_{ij} > r_0$.

The graph of Morse Potential see figure 5.1 shows that the characteristics of the flocking are satisfied. Therefore it will be instructive to add Morse Potential to our generalized model.

In this section, we consider the closed-loop model, and we add the force derived from Morse Potential. Indeed, the force derived from this energy is the gradient of $U(r)$, that is:

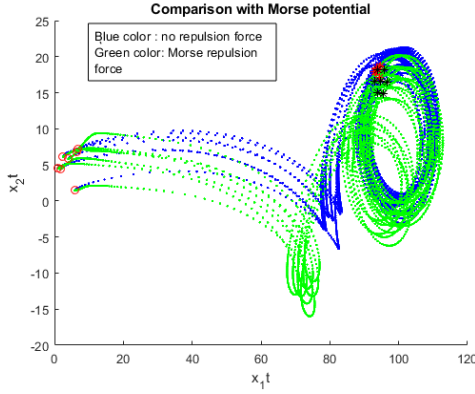
$$F(r) = -\frac{\partial U}{\partial r}u = -2D a \exp(-a(r_{ij} - r_0))(1 - \exp(-a(r_{ij} - r_0)))u$$

Where D , a are positive constants and will be picked systematically for our simulation, and u is a unit vector along the line joining the two agents. The model reads as follows.

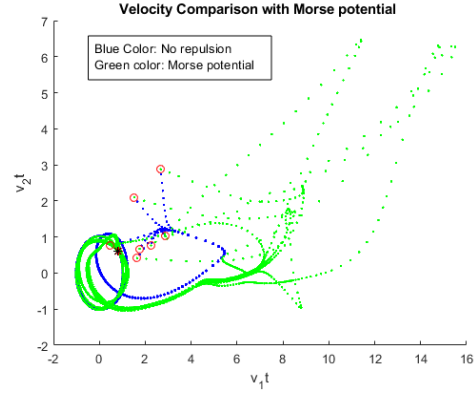
$$\begin{aligned}\frac{dx_i}{dt} &= v_i \\ \frac{dv_i}{dt} &= \alpha_i(t)(\bar{v}_i - v_i) + \beta_i(t) \\ &\quad + \frac{1}{N} \sum_{j=1}^N -2D a \exp(-a(r_{ij} - r_0))(1 - \exp(-a(r_{ij} - r_0))) \frac{x_j - x_i}{r_{ij}}.\end{aligned}\tag{5.1.1}$$

To discern the effect of the MP force, we will keep the same initial conditions and the same target trajectory that we have used in Chapter 4 for simulations. Figures 5.2 show the effect of the added forces. In these graphs, the blue color corresponds to the model without repulsion forces; we refer to it as the first model, while the green color represents the output of the model with the repulsion forces. We will call it the second model. The open red circles represent the initial position in both trajectory and velocity space. Red stars represent the final position for the first model, and black stars represent the final position for the second model. The figure 5.2b shows that when the Morse potential force is added, it has a significant effect at the beginning. We can see that the green and the blue trajectories are not similar. In fact, while in the first model, all velocities seem to move towards an interior point of the convex hull formed by their initial position, in the second model, we see that some agents move away from that convex hull. In both models, we can observe that all agents agree at the same velocity and then steer towards the target velocity. The effect of the MP forces is also seen in the trajectory space. Indeed, we have that in

both models, we start at the same initial positions, but we have different paths. We can also see that in figure 5.2a the red stars are very close together while the black stars are not. This can be further justified by the minimum distance graph between agents in both models. In fact, in figure 5.3 we see that the minimum distance decreases on the first model while it increases faster on the second model until a value close to $r = 1.8$. The parameter values for our simulation are: $D = 16$, $r_0 = 2$ and $a = 1.2$



(a) Comparison in the trajectory space



(b) Comparison in velocity space

Figure 5.2: Comparison of solutions $x_i(t)$ and $v_i(t)$: Case of Morse potential

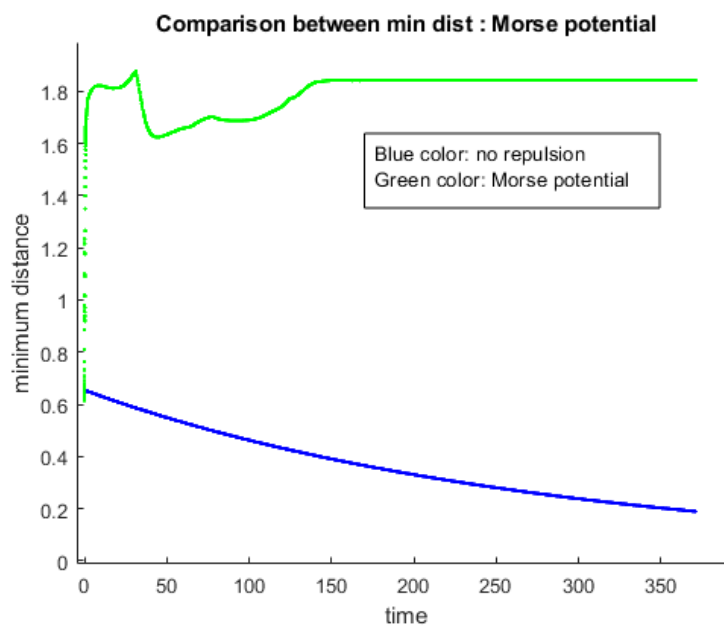


Figure 5.3: Comparison minimum distance between agents: case of Morse potential(green), case without repulsion (blue)

5.2 Simulation of the Model with Inter-particle Bonding Forces

In [27] Park et al develop via some heuristic method two forces T_1 and T_2 given by,

$$T_1 = \frac{1}{N} \sum_{j=1}^N \frac{K_1}{2r_{ij}^2} \langle v_i - v_j, x_i - x_j \rangle (x_j - x_i),$$

$$T_2 = \frac{1}{N} \sum_{j=1}^N \frac{K_2}{2r_{ij}} (r_{ij} - 2r_0) (x_j - x_i).$$

Here, the vector T_1 guarantees cohesion, and the vector T_2 guarantees collision avoidance. K_1 and K_2 are two positive constant. Park et al show that when the CS model is augmented by these two forces, the resulting model flocks and agents can maintain a minimum distance close to $2r_0$ from each other. Following the same idea, we add these forces to our generalized model and numerically describe their effect on the model. The new model under consideration is

$$\begin{aligned} \frac{dx_i}{dt} &= v_i \\ \frac{dv_i}{dt} &= \alpha_i(t)(\bar{v}_i - v_i) + \beta_i(t) + \frac{1}{N} \sum_{j=1}^N \frac{K_1}{2r_{ij}^2} \langle v_i - v_j, x_i - x_j \rangle (x_j - x_i) \\ &\quad + \frac{1}{N} \sum_{j=1}^N \frac{K_2}{2r_{ij}} (r_{ij} - 2r_0) (x_j - x_i). \end{aligned} \quad (5.2.1)$$

Here, $2r_0$ represents the desired minimum distance between agents. Thus r_0 will be our control parameter. $r_{ij} = \|x_i - x_j\|$. K_1 and K_2 are fixed parameters which will be choose systematically.

We simulate our ameliorated model with the following parameters: $2r_0 = 2$ is the desired minimum distance that we want to maintain between agents. $K_1 = 30$

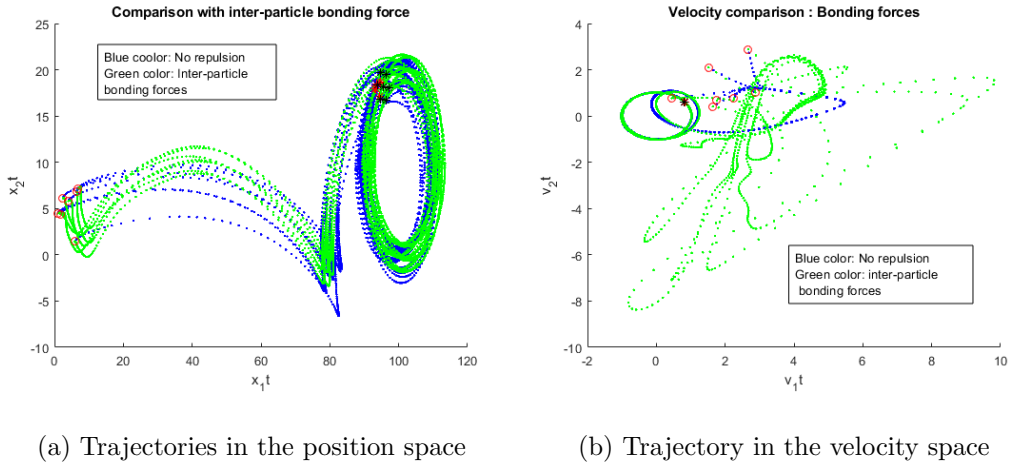


Figure 5.4: Comparison of solution x_i and v_i : Case of inter-particle bonding forces

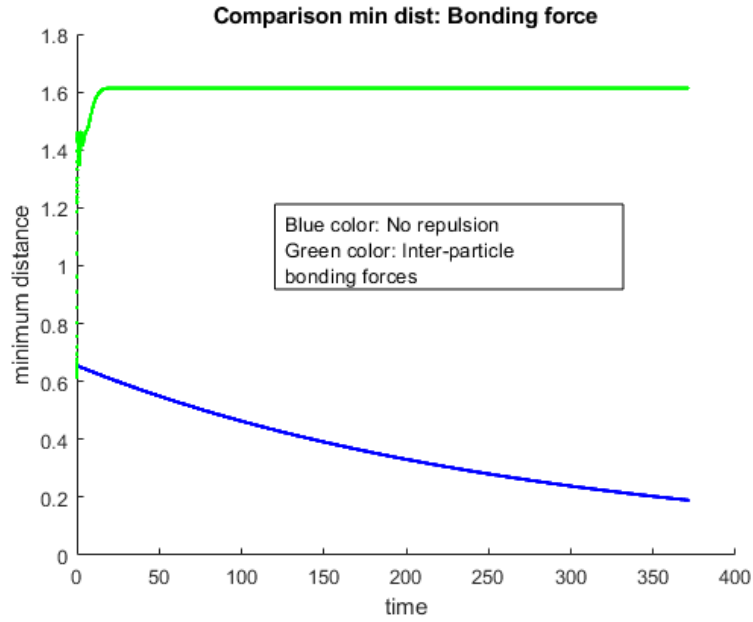


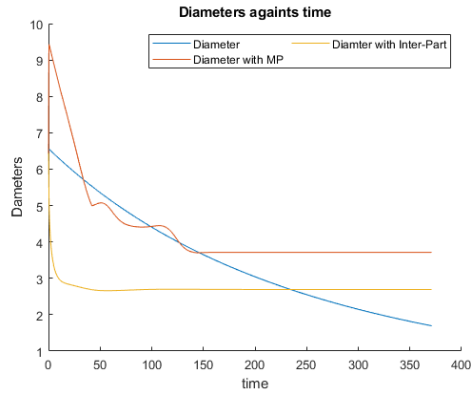
Figure 5.5: Comparison of minimum distance when the inter-particle bonding force is added.

and $K_2 = 50$. The figures 5.4 and 5.5 have the same interpretation as in the case of Morse potential forces. We see that there are discrepancies in trajectories in position and velocity space. We see alignment in the velocity space figure 5.4b. Since all velocities align and then steer towards the target velocity. The effect of these forces can also be seen in the position space. In figure 5.4 we see that both models start with the same initial condition but do not follow the same path. We can further see that the red stars are close to each other compared to the black stars which maintain some minimum distance between agents. To emphasize this observation, we draw the minimum distance graph in both models, see figure 5.5. In this figure, the initial minimum distance is 0.6. In the second model, the minimum distance increases faster until a value of 1.6. This suggests that for a good choice of parameters, collisions can be avoided.

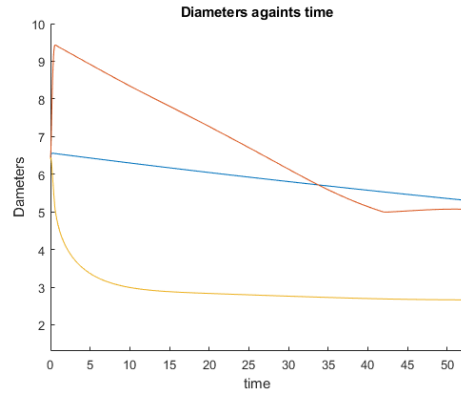
In this chapter, we presented the effect of repulsive forces on our generalized model with steering. We saw that in both cases, with a good selection of parameters of the model, we can achieve collision avoidance. In the case of Morse potential forces, we saw that at the initial time $t = 0$ the minimum distance is 0.6 which is less than $r_0 = 2$. The Morse Potential forces act as repulsive forces and agents move away from each other. This effect can be seen in figure 5.2b. The same scenario is observed in the case of inter-particle bonding forces which is also depicted graphically in figure 5.4b. We also have that the minimum distance at the equilibrium is less

than $r_0 = 2$ as we want. This may be due to the fact that there are many agents exerting external forces on agent i . We further plot the diameters $d_X(t)$ and $d_V(t)$ as a function of time see Figures 5.6 and 5.7.

In these figures, the red color represents the case of Morse potential forces, the orange color represents the case of inter-particle bonding forces and the blue color is the case without any forces. From these graphs, we read that the Morse potential forces create a strong disturbance in the model. Indeed, $d_X(t)$ increases rapidly at the beginning to a large value then decreases and becomes constant around a value of 4. In the case of inter-particle bonding forces, $d_X(t)$ behaves nicely. We can see that the orange graph decreases smoothly and becomes constant around a value of 3. From figure 5.7, we read that the Morse potential forces create a strong disturbance in the velocity space compared to the case of inter-particle bonding forces. We also see that the diameter $d_V(t)$ goes to zero faster when the Morse potential forces are added. In the case of inter-particle bonding forces, $d_V(t)$ does not increase as fast as the case of Morse potential forces. We can also see that $d_V(t)$ does not go to zero faster.

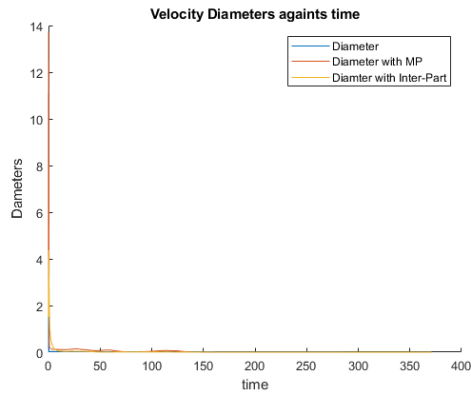


(a) long simulation

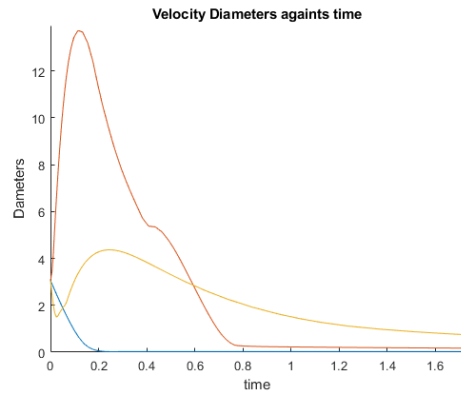


(b) short simulation

Figure 5.6: Comparison of the configuration diameters of the model: Diameter without a repulsive force (blue). Diameter with Morse Potential(red). Diameter with inter-particle bonding forces(orange)



(a) long simulation



(b) short simulation

Figure 5.7: Comparison of diameters velocity of the model: Diameter without a repulsive force (blue). Diameter with Morse Potential(red). Diameter with inter-particle bonding forces(orange)

Chapter 6: Conclusion

We introduced and analyzed a generalized model of flocking with steering. In our model, the acceleration of each agent has flocking and steering components. The flocking component is a generalization of many existing models and takes into account real-world factors such as apriori bound on acceleration, masking effects, and orientation bias. We further improved the model by adding to each agent's acceleration, a steering term that allows to capture the whims of that agent. We provided examples of a function with acceleration bound and an influence function with masking effect. Under some suitable assumptions, we showed the existence and uniqueness of the model's solution and we also proved that the maximal interval of existence is $[0, \infty)$. We proved that our generalized model with steering flocks under certain sufficient conditions which naturally include assumptions on the steering components $\beta_i(t)$ of the accelerations of the agents. Note that our analysis did not suggest flocking with a constant velocity as in the case of most existing models. This was confirmed by simulation in which we can see that the asymptotic velocity is not constant in time. We also studied the case where flocking is much faster than

steering using formal singular perturbation theory and showed that the leading order behavior is one where the agents flock together with velocity v^f which evolves in time, see (4.1.14). Our simulations showed that the leading order approximation was very similar to the real solution for small values of ϵ a scale parameter indicating the magnitude difference between flocking and steering accelerations. We gave in Section 4.4 a rigorous proof that shows that a singularly perturbed model flocks when $\epsilon \rightarrow 0$ and $t \in (0, T)$ with $T < \infty$.

In order to avoid collision in our generalized flocking model with steering, we further ameliorated this model by incorporating extra forces. First, we augmented the acceleration of each agent by forces derived from Morse Potential, and with inter-particle bonding forces secondly. Simulations suggested that for a good choice of parameters of the model, collisions may be prevented.

We also observed that the influence function ϕ_{ij} were assumed to be nonvanishing for all $i, j \in 1, \dots, N$ in our flocking results. This implies that the communication graph formed by the agents is strongly connected. In the case of robotic systems, this will be computationally expensive. Even in the case of biological agents, all to all communication among agents may not be a reasonable assumption. This raises the question of whether one could relax the strict positivity condition and still obtain flocking results.

Our flocking results assumed that the steering components $\beta_i(t)$ of the agents were asymptotically in agreement ($\beta_i(t) - \beta_j(t) \rightarrow 0$ as $t \rightarrow \infty$). A related natural

question is if the agents form subgroups within which this condition holds but fails across these subgroups, then can we obtain clusters of agents such that agents within each cluster flock together.

Appendix A: Useful Lemmas

Lemma 5 *Let $F : \mathbb{R}^d \rightarrow \mathbb{R}$ be locally Lipschitz and $u : [0, T] \rightarrow \mathbb{R}^d$ be absolutely continuous. Then $F \circ u : [0, T] \rightarrow \mathbb{R}$ is absolutely continuous.*

Proof Since F is locally Lipschitz and $u([0, T])$ is compact in \mathbb{R}^d , there exists $K > 0$ such that

$$|F(a) - F(b)| \leq K\|a - b\|$$

for all a, b in \mathbb{R}^d . Let $\epsilon > 0$. Since u is absolutely continuous, there exist $\delta > 0$ such that for every n

$$\sum_{i=1}^n |u(t_i) - u(s_i)| < \frac{\epsilon}{K}$$

whenever

$$\sum_{i=1}^n |t_i - s_i| < \delta,$$

where $[t_i, s_i]$ is a finite collection of mutually disjoint sub intervals of $[0, T]$. Hence

$$\sum_{i=1}^n |(F \circ u)(t_i) - (F \circ u)(s_i)| = \sum_{i=1}^n |F(u(t_i)) - F(u(s_i))| \leq K \sum_{i=1}^n |u(t_i) - u(s_i)| < \epsilon.$$

■

Lemma 6 *The function $F : \mathbb{R}^n \rightarrow \mathbb{R}$ defined by*

$$F(x) = \max\{x_i \mid i = 1 \dots n\}$$

is Lipschitz.

Proof $|F(x) - F(y)| = |\max_i x_i - \max_i y_i| \leq \max_i |x_i - y_i| \leq \|x - y\|.$ ■

Lemma 7 *Let $f_i : \mathbb{R} \rightarrow \mathbb{R}$ be absolutely continuous on $[0, T]$ for $i = 1, \dots, n$ and let $f : \mathbb{R} \rightarrow \mathbb{R}$ be defined by*

$$f(t) = \max\{f_i(t) \mid i = 1 \dots n\}.$$

Suppose $i_ : \mathbb{R} \rightarrow \{1, \dots, n\}$ satisfies $f_{i_*(t)}(t) \geq f_j(t)$ for all t and $j = 1, \dots, n$.*

Then f is absolutely continuous and $f'(t) = f'_{i_(t)}(t)$ for almost all t .*

Proof f_i are absolutely continuous and the max function is Lipschitz. Then by Lemma 5 f is absolutely continuous. Therefore, f is differentiable almost everywhere.

Now let us compute f' . f differentiable almost everywhere, therefore there exist a measurable set $G \subset (0, T)$ such that $((0, T) \setminus G)$ has a zero measure and f, f_1, \dots, f_N are differentiable on G . Let $t^* \in G$ and let i satisfying $f(t^*) = f_i(t^*)$ we shall show that $f'(t^*) = f'_i(t^*)$. We have for $t \geq t^*$

$$\frac{f(t) - f(t^*)}{t - t^*} \geq \frac{f_i(t) - f_i(t^*)}{t - t^*}$$

taking the limit from the right of t^* we have

$$\lim_{t \rightarrow t^{*+}} \frac{f(t) - f(t^*)}{t - t^*} \geq \lim_{t \rightarrow t^{*+}} \frac{f_i(t) - f_i(t^*)}{t - t^*},$$

this reads

$$f'(t^*) \geq f'_i(t^*).$$

On the other hand, for $t \leq t^*$

$$\frac{f(t) - f(t^*)}{t - t^*} \leq \frac{f_i(t) - f_i(t^*)}{t - t^*}$$

taking the limit from the left of t^* we have

$$\lim_{t \rightarrow t^{*-}} \frac{f(t) - f(t^*)}{t - t^*} \leq \lim_{t \rightarrow t^{*-}} \frac{f_i(t) - f_i(t^*)}{t - t^*},$$

this reads

$$f'(t^*) \leq f'_i(t^*).$$

It come that $f'(t) = f'_i(t)$ for all $t \in G$. ■

Lemma 8 *The forward maximal interval of existence of the open-loop model 2.6.1 and the closed-loop model 2.6.2 is $[0, \infty)$ where we assume that Assumptions 3, 2, 1 hold.*

Proof Let us suppose that the forward maximal interval of existence is $[0, T^*)$, with $T^* < \infty$. We define the energy of the system by $E(t) = \max_i E_i(t) = \max_i \frac{1}{2} \|v_i(t)\|^2$.

Then

$$\begin{aligned} \frac{dE(t)}{dt} &= \langle v_i, \dot{v}_i \rangle = \langle v_i, \alpha_i(\bar{v}_i - v_i) + \beta_i \rangle \\ &= \alpha_i \langle v_i, \bar{v}_i \rangle - \alpha_i \langle v_i, v_i \rangle + \alpha_i \langle v_i, \beta_i \rangle \\ &\leq \alpha_i \|v_i\| \left(\sum_j a_{ij} \|v_j\| \right) - \alpha_i \|v_i\|^2 + \alpha_i \|v_i\| \|\beta_i\| \\ &\leq \alpha_i \|v_i\| \|\beta_i\| \end{aligned}$$

We have used the Cauchy-Schwartz inequality and the conditions $\|v_j\| \leq \|v_i\|$ and $\sum_j a_{ij} = 1$. We rearrange this inequality to

$$\frac{dE(t)}{dt} \leq \alpha_i (2E(t))^{\frac{1}{2}} \|\beta_i\| \leq \bar{\alpha} (2E(t))^{\frac{1}{2}} \|\beta_i\|. \quad (\text{A.0.1})$$

Where $\bar{\alpha}$ is the maximum of $\alpha_i(t)$ over i and $t \in [0, T^*]$ in the case of open-loop. In the case of closed-loop model, $\alpha_i(t) = \xi_i(\bar{v}_i - v_i)$, where the ξ_i satisfy Assumption 1.

We have that , ξ_i are continuous function therefore

$$\begin{aligned} \lim_{\|u\| \rightarrow 0} \xi_i(u) &= \lim_{u \rightarrow 0} \xi_i(u) = \xi_i(0) \\ \lim_{\|u\| \rightarrow \infty} \xi_i(u) &\leq \lim_{\|u\| \rightarrow \infty} \frac{A}{\|u\|} = 0. \end{aligned}$$

we can deduce that there exist a positive constant K_i such that

$$\xi_i(u) \leq K_i \quad \forall u \in \mathbb{R}^d$$

So, in the case of closed-loop, take $\bar{\alpha}$ to be the maximum value of K_i . Multiplying the inequality A.0.1 by $(2E(t))^{-\frac{1}{2}}$ we may obtain

$$\frac{dE^{\frac{1}{2}}(t)}{dt} \leq 2^{\frac{1}{2}} \bar{\alpha} \|\beta_i\|.$$

Let $M_\beta > 0$ satisfy $\|\beta_i(t)\| \leq M_\beta$ for all i and $t \in [0, T^*]$. We obtain

$$\left(E^{\frac{1}{2}}(t) - E^{\frac{1}{2}}(0) \right) \leq 2^{-\frac{1}{2}} \bar{\alpha} M_\beta T^*.$$

And we deduce that

$$\|v_i\| \leq \left(E^{\frac{1}{2}}(0) + 2^{-\frac{1}{2}} \bar{\alpha} M_\beta T^* \right) < \infty.$$

We then deduce the upper bound of the vector position $x_i(t)$ as

$$\|x_i(t)\| \leq \left(E^{\frac{1}{2}}(0) + 2^{-\frac{1}{2}} \bar{\alpha} M_\beta T^* \right) T^* + \|x_i(0)\|.$$

Since the solution remains in a compact set for $t \in [0, T^*)$ we obtain a contradiction. ■

In the following lemma, we suppose that the steering vector is giving by:

$$\beta_i(t) = \alpha_1 v_i(t) + \alpha_2 x_i(t) + \gamma_i(t). \quad (\text{A.0.2})$$

Where α_1 and α_2 are positive real numbers, $\gamma_i(t) \in \mathcal{C}([0, \infty); \mathbb{R}^d)$. We also define the following norm:

$$\|(x_1, \dots, x_N)\|_\infty = \max_{1 \leq i \leq N} \|x_i\|.$$

Lemma 9 *The forward maximal interval of existence of the model (2.6.2) in which β_i is giving by (A.0.2) is $[0, \infty)$ where we assume that γ_i are continuous on $[0, \infty)$.*

Proof Let $(x_i, v_i)_{i=1}^N$ be the solution of our closed-loop model. We assume that solution are absolutely continuous. Using the norm defined above, we see that

$$\begin{aligned} \frac{d}{dt} \|x\|_\infty &\leq \|v\|_\infty, \\ \frac{d}{dt} \|v\|_\infty &\leq \|\beta\|_\infty. \end{aligned}$$

Let $[0, T)$ be the maximum interval of existence, where $T < \infty$ of 2.6.2. We have

$$\|\beta\|_\infty(t) \leq \alpha_1 \|v_k(t)\| + \alpha_2 \|x_k(t)\| + \|\gamma_i(t)\| \leq \alpha_1 \|v(t)\|_\infty + \alpha_2 \|x(t)\|_\infty + \|\gamma_i(t)\|.$$

for some k such that $\max_i \|\beta_i\| = \|\beta_k\|$. Which implies that

$$\begin{aligned}\frac{d}{dt}\|x\|_\infty &\leq \|v\|_\infty \\ \frac{d}{dt}\|v\|_\infty &\leq \alpha_1\|v\|_\infty + \alpha_2\|x\|_\infty + \|\gamma(t)\|.\end{aligned}\tag{A.0.3}$$

Since x_i and v_i are absolutely continuous, using Lemma 5, $\|v\|_\infty$ and $\|x\|_\infty$ are absolutely continuous. The first inequality is

$$\frac{d}{dt}\|x\|_\infty \leq \|v\|_\infty.$$

Which solves to

$$\|x(t)\|_\infty - \|x(0)\|_\infty \leq \int_0^t \|v(s)\|_\infty ds.\tag{A.0.4}$$

Replacing (A.0.4), in the second inequality of (A.0.3) and there exist K such that

$\|\gamma_i(t)\| \leq K$ for $t \in (0, T]$ we obtain

$$\begin{aligned}\frac{d}{dt}\|v\|_\infty &\leq \alpha_1\|v\|_\infty + \alpha_2\|x\|_\infty + \|\gamma(t)\| \\ &\leq \alpha_1\|v\|_\infty + \alpha_2 \int_0^t \|v(s)\|_\infty ds + \alpha_2\|x(0)\| + K.\end{aligned}$$

That is

$$\begin{aligned}\|v(t)\|_\infty &\leq \|v(0)\|_\infty + \int_0^t \alpha_1\|v(s)\|_\infty ds + \alpha_2 \int_0^t \int_0^s \|v(r)\|_\infty dr ds + \int_0^t (K + \alpha_2\|x(0)\|_\infty) ds \\ &\leq \|v(0)\|_\infty + \int_0^t \alpha_1\|v(s)\|_\infty ds + \int_0^t \alpha_1 \int_0^s \frac{\alpha_2}{\alpha_1} \|v(r)\|_\infty dr ds + \int_0^t (K + \alpha_2\|x(0)\|_\infty) ds.\end{aligned}$$

Using the generalized Gronwall inequality in [26] where $f(s) = \alpha_1$ and $g(s) = \frac{\alpha_2}{\alpha_1}$,

we have the following inequality on $\|v(t)\|_\infty$

$$\begin{aligned}\|v(t)\|_\infty &\leq \|v(0)\|_\infty \left(1 + \int_0^t \alpha_1 \exp \left(\int_0^s (\alpha_1 + \frac{\alpha_2}{\alpha_1}) dr \right) ds \right) + \int_0^t (K + \alpha_2\|x(0)\|_\infty) ds \\ &\leq \|v(0)\|_\infty \left(1 + \int_0^t \alpha_1 \exp \left(\int_0^s (\alpha_1 + \frac{\alpha_2}{\alpha_1}) dr \right) ds \right) + K_1 t.\end{aligned}\tag{A.0.5}$$

Where $K_1 = K + \alpha_2 \|x(0)\|_\infty$. That gives,

$$\begin{aligned} \|v(t)\|_\infty &\leq \|v(0)\|_\infty \left(1 + \alpha_1 \left(\alpha_1 + \frac{\alpha_2}{\alpha_1} \right)^{-1} \left(\exp \left(\alpha_1 + \frac{\alpha_2}{\alpha_1} \right) t - 1 \right) \right) + K_1 t \\ &\leq \|v(0)\|_\infty \left(1 + \alpha_1 \left(\alpha_1 + \frac{\alpha_2}{\alpha_1} \right)^{-1} \left(\exp \left(\alpha_1 + \frac{\alpha_2}{\alpha_1} \right) T - 1 \right) \right) + K_1 T \quad \forall t \in [0, T]. \end{aligned}$$

It comes that for $t \in [0, T)$, $\|v_i(t)\|$ is bounded whenever $t \in [0, T)$ that is

$$\|v_i\| \leq \|v(0)\|_\infty \left(1 + \alpha_1 \left(\alpha_1 + \frac{\alpha_2}{\alpha_1} \right)^{-1} \left(\exp \left(\alpha_1 + \frac{\alpha_2}{\alpha_1} \right) T - 1 \right) \right) + K_1 T \quad (\text{A.0.6})$$

From (A.0.4) we deduce that,

$$\|x_i\| \leq \|x(t)\| \leq \|x(0)\|_\infty + \|v(0)\|_\infty \left(1 + \alpha_1 \left(\alpha_1 + \frac{\alpha_2}{\alpha_1} \right)^{-1} \left(\exp \left(\alpha_1 + \frac{\alpha_2}{\alpha_1} \right) T - 1 \right) \right) T + K_1 T^2 \quad (\text{A.0.7})$$

Since the solution remains in a compact set for $t \in [0, T)$, we obtain a contradiction.

■

Bibliography

- [1] S. M. Ahn, H. Choi, S.-Y. Ha, and H. Lee, “On collision-avoiding initial configurations to cuckoo-smale type flocking models”, *Communications in Mathematical Sciences*, vol. 10, no. 2, pp. 625–643, 2012.
- [2] S. M. Ahn and S.-Y. Ha, “Stochastic flocking dynamics of the cuckoo-smale model with multiplicative white noises”, *Journal of Mathematical Physics*, vol. 51, no. 10, p. 103301, 2010.
- [3] G. Albi, D. Balagué, J. A. Carrillo, and J. von Brecht, “Stability analysis of flock and mill rings for second order models in swarming”, *SIAM Journal on Applied Mathematics*, vol. 74, no. 3, pp. 794–818, 2014.
- [4] M. Aureli and M. Porfiri, “Coordination of self-propelled particles through external leadership”, *EPL (Europhysics Letters)*, vol. 92, no. 4, p. 40004, 2010.
- [5] H.-O. Bae, Y.-P. Choi, S.-Y. Ha, and M.-J. Kang, “Asymptotic flocking dynamics of cuckoo-smale particles immersed in compressible fluids”, *Discrete Contin. Dyn. Syst.*, vol. 34, no. 11, pp. 4419–4458, 2014.
- [6] M. Bongini, M. Fornasier, and D. Kalise, “Emergence under perturbed and decentralized feedback controls”, 2014.
- [7] J. A. Canizo, J. A. Carrillo, and J. Rosado, “A well-posedness theory in measures for some kinetic models of collective motion”, *Mathematical Models and Methods in Applied Sciences*, vol. 21, no. 03, pp. 515–539, 2011.
- [8] M. Caponigro, M. Fornasier, B. Piccoli, and E. Trélat, “Sparse stabilization and control of alignment models”, *Mathematical Models and Methods in Applied Sciences*, vol. 25, no. 03, pp. 521–564, 2015.
- [9] J. A. Carrillo, A. Klar, S. Martin, and S. Tiwari, “Self-propelled interacting particle systems with roosting force”, *Mathematical Models and Methods in Applied Sciences*, vol. 20, no. supp01, pp. 1533–1552, 2010.
- [10] J. B. Clark and D. R. Jacques, “Flight test results for uavs using boid guidance algorithms”, *Procedia Computer Science*, vol. 8, pp. 232–238, 2012.
- [11] F. Cucker and J.-G. Dong, “Avoiding collisions in flocks”, *IEEE Transactions on Automatic Control*, vol. 55, no. 5, pp. 1238–1243, 2010.

- [12] F. Cucker, S. Smale, *et al.*, “Emergent behavior in flocks”, *IEEE Transactions on automatic control*, vol. 52, no. 5, pp. 852–862, 2007.
- [13] F. Cucker and S. Smale, “On the mathematics of emergence”, *Japanese Journal of Mathematics*, vol. 2, no. 1, pp. 197–227, 2007.
- [14] M. R. D’Orsogna, Y.-L. Chuang, A. L. Bertozzi, and L. S. Chayes, “Self-propelled particles with soft-core interactions: Patterns, stability, and collapse”, *Physical review letters*, vol. 96, no. 10, p. 104302, 2006.
- [15] V. Gazi and K. M. Passino, “Stability analysis of swarms”, *IEEE transactions on automatic control*, vol. 48, no. 4, pp. 692–697, 2003.
- [16] S.-Y. Ha, T. Ha, and J.-H. Kim, “Emergent behavior of a cucker-smale type particle model with nonlinear velocity couplings”, *IEEE Transactions on Automatic Control*, vol. 55, no. 7, pp. 1679–1683, 2010.
- [17] S.-Y. Ha, K. Lee, D. Levy, *et al.*, “Emergence of time-asymptotic flocking in a stochastic cucker-smale system”, *Communications in Mathematical Sciences*, vol. 7, no. 2, pp. 453–469, 2009.
- [18] S.-Y. Ha, J.-G. Liu, *et al.*, “A simple proof of the cucker-smale flocking dynamics and mean-field limit”, *Communications in Mathematical Sciences*, vol. 7, no. 2, pp. 297–325, 2009.
- [19] S.-Y. Ha and E. Tadmor, “From particle to kinetic and hydrodynamic descriptions of flocking”, *arXiv preprint arXiv:0806.2182*, 2008.
- [20] J. Haskovec, “Flocking dynamics and mean-field limit in the cucker-smale-type model with topological interactions”, *Physica D: Nonlinear Phenomena*, vol. 261, pp. 42–51, 2013.
- [21] J. M. Hendrickx and J. N. Tsitsiklis, “Convergence of type-symmetric and cut-balanced consensus seeking systems”, *IEEE Transactions on Automatic Control*, vol. 58, no. 1, pp. 214–218, 2013.
- [22] A. Jadbabaie, J. Lin, and A. S. Morse, “Coordination of groups of mobile autonomous agents using nearest neighbor rules”, *IEEE Transactions on automatic control*, vol. 48, no. 6, pp. 988–1001, 2003.
- [23] C.-H. Li and S.-Y. Yang, “A new discrete cucker-smale flocking model under hierarchical leadership”, *Discrete & Continuous Dynamical Systems-B*, vol. 21, no. 8, p. 2587, 2016.
- [24] L. Li, L. Huang, and J. Wu, “Flocking and invariance of velocity angles”, *Mathematical Biosciences & Engineering*, vol. 13, no. 2, p. 369, 2016.
- [25] S. Motsch and E. Tadmor, “A new model for self-organized dynamics and its flocking behavior”, *Journal of Statistical Physics*, vol. 144, no. 5, p. 923, 2011.

- [26] B. Pachpatte, “A note on gronwall-bellman inequality”, *Journal of Mathematical Analysis and Applications*, vol. 44, no. 3, pp. 758–762, 1973.
- [27] J. Park, H. J. Kim, and S.-Y. Ha, “Cucker-smale flocking with inter-particle bonding forces”, *IEEE Transactions on Automatic Control*, vol. 55, no. 11, pp. 2617–2623, 2010.
- [28] L. Perea, G. Gómez, and P. Elosegui, “Extension of the cucker-smale control law to space flight formations”, *Journal of guidance, control, and dynamics*, vol. 32, no. 2, pp. 527–537, 2009.
- [29] C. W. Reynolds, “Flocks, herds and schools: A distributed behavioral model”, vol. 21, no. 4, pp. 25–34, 1987.
- [30] J. Shen, “Cucker–smale flocking under hierarchical leadership”, *SIAM Journal on Applied Mathematics*, vol. 68, no. 3, pp. 694–719, 2008.
- [31] S. T. Stamoulas and M. Rathinam, “Convergence, stability, and robustness of multidimensional opinion dynamics in continuous time”, *SIAM Journal on Control and Optimization*, vol. 56, no. 3, pp. 1938–1967, 2018.
- [32] T. Vicsek, A. Czirók, E. Ben-Jacob, I. Cohen, and O. Shochet, “Novel type of phase transition in a system of self-driven particles”, *Physical review letters*, vol. 75, no. 6, p. 1226, 1995.

